Persoonia 44, 2020: 41–66
www.ingentaconnect.com/content/nhn/pimj

RESEARCH ARTICLE

ISSN (Online) 1878-9080
https://doi.org/10.3767/persoonia.2020.44.02

Patterns of coevolution between ambrosia beetle mycangia and the *Ceratocystidaceae*, with five new fungal genera and seven new species

C.G. Mayers[1], T.C. Harrington[1], H. Masuya[2], B.H. Jordal[3], D.L. McNew[1], H.-H. Shih[4], F. Roets[5], G.J. Kietzka[5]

Key words

14 new taxa
Microascales
Scolytinae
symbiosis
two new typifications

Abstract Ambrosia beetles farm specialised fungi in sapwood tunnels and use pocket-like organs called mycangia to carry propagules of the fungal cultivars. Ambrosia fungi selectively grow in mycangia, which is central to the symbiosis, but the history of coevolution between fungal cultivars and mycangia is poorly understood. The fungal family *Ceratocystidaceae* previously included three ambrosial genera (*Ambrosiella*, *Meredithiella*, and *Phialophoropsis*), each farmed by one of three distantly related tribes of ambrosia beetles with unique and relatively large mycangium types. Studies on the phylogenetic relationships and evolutionary histories of these three genera were expanded with the previously unstudied ambrosia fungi associated with a fourth mycangium type, that of the tribe *Scolytoplatypodini*. Using ITS rDNA barcoding and a concatenated dataset of six loci (28S rDNA, 18S rDNA, *tef*1-α, *tub*, *mcm7*, and *rpl1*), a comprehensive phylogeny of the family *Ceratocystidaceae* was developed, including *Inodoromyces interjectus* gen. & sp. nov., a non-ambrosial species that is closely related to the family. Three minor morphological variants of the pronotal disk mycangium of the *Scolytoplatypodini* were associated with ambrosia fungi in three respective clades of *Ceratocystidaceae*: *Wolfgangiella* gen. nov., *Toshionella* gen. nov., and *Ambrosiella remansi* sp. nov. Closely-related species that are not symbionts of ambrosia beetles are accommodated by *Catunica adiposa* gen. & comb. nov. and *Solaloca norvegica* gen. & comb. nov. The divergent morphology of the ambrosial genera and their phylogenetic placement among non-ambrosial genera suggest three domestication events in the *Ceratocystidaceae*. Estimated divergence dates for the ambrosia fungi and mycangia suggest that *Scolytoplatypodini* mycangia may have been the first to acquire *Ceratocystidaceae* symbionts and other ambrosial fungal genera emerged shortly after the evolution of new mycangium types. There is no evidence of reversion to a non-ambrosial lifestyle in the mycangial symbionts.

Article info Received: 5 November 2018; Accepted: 4 March 2019; Published: 29 July 2019.

INTRODUCTION

Multiple groups of wood-boring weevils, collectively known as ambrosia beetles, cultivate fungal gardens along the walls of their sapwood tunnels (‘galleries’) in a reciprocally obligate mutualism (Hulcr & Stelinski 2017). The dozen or more separately-evolved lineages of ambrosia beetles (Kirkendall et al. 2015, Hulcr & Stelinski 2017) avoid competition from phloem-feeding bark beetles and other insects in the nutritious inner bark by using fungal agriculture to exploit the nutrient-poor sapwood (Harrington 2005, Harrington et al. 2010). Reciprocally-obligate fungus farming is shared with only two other lineages of insects: the higher-attine ants (Mueller et al. 2018) and the *Termitomyces*-farming termites (Nobre et al. 2011), but ambrosia beetles are unique in their use of special fungus-carrying pockets called mycangia that allow cultivar persistence across generations (Francke-Grosmann 1956, 1963, 1967). The fungi benefit from targeted transport to fresh substrate in mycangia, and they are also protected from desiccation; ambrosia fungi appear to be unable to disperse and survive independently. Mycangia are central to the ambrosia beetle-fungus symbiosis, and they drive the evolution of both ambrosia beetles and the fungi that grow inside them.

The term mycangium is broadly applied to a range of separately-evolved physical adaptations (usually invaginations of the exoskeleton that form pockets, cavities, or crevices) on different parts of the beetles’ bodies for the storage and transport of fungal spores (Francke-Grosmann 1963, 1967, Beaver 1989, Six 2003). The most effective and selective mycangia are ‘glandular sac mycangia’ (Six 2003) associated with active gland cells that secrete nutrients into or near the mycangium lumen (Schedl 1962, Francke-Grosmann 1963, 1967). The secretions support the selective, asexual growth of fungal symbionts (Schneider 1975, Skelton et al. 2019), and the propagules overflow from the mycangium opening to inoculate galleries during sapwood excavation (Schedl 1962, Beaver 1989, Harrington et al. 2014). Most mycangia are small relative to the beetles’ body size (hereafter ‘small mycangia’) and are relatively simple in structure, such as the oral/preoral pouch mycangia convergently developed by multiple ambrosia beetle lineages (Hulcr & Stelinski 2017). Certain other mycangia are larger internal cavities with more complex structure (hereafter ‘large mycangia’). Large mycangia are believed to represent

[1] Department of Plant Pathology and Microbiology, Iowa State University, 2213 Pammel Drive, 1344 Advanced Teaching and Research Building, Ames, Iowa, 50011, USA; present address: Plant Pathology and Plant-Microbe Biology Section, Cornell University, 412 Bradfield Hall, Ithaca, New York, 14850, USA; corresponding author e-mail: chasemayers@gmail.com.
[2] Department of Forest Microbiology, Forestry & Forest Products Research Institute (FFPRI), 1 Matsunosato, Tsukuba, Ibaraki 305-8687, Japan.
[3] University Museum of Bergen, PB 7800, NO-5020 Bergen, Norway.
[4] Taiwan Forestry Research Institute, No. 53 Nanhai Rd., Zhongzheng Dist., Taipei City 10066, Taiwan.
[5] Department of Conservation Ecology and Entomology, Stellenbosch University, Stellenbosch, 7600, South Africa.

© 2019-2020 Naturalis Biodiversity Center & Westerdijk Fungal Biodiversity Institute

You are free to share - to copy, distribute and transmit the work, under the following conditions:
Attribution: You must attribute the work in the manner specified by the author or licensor (but not in any way that suggests that they endorse you or your use of the work).
Non-commercial: You may not use this work for commercial purposes.
No derivative works: You may not alter, transform, or build upon this work.
For any reuse or distribution, you must make clear to others the license terms of this work, which can be found at http://creativecommons.org/licenses/by-nc-nd/3.0/legalcode. Any of the above conditions can be waived if you get permission from the copyright holder. Nothing in this license impairs or restricts the author’s moral rights.

Table 1 Collection information and ITS rDNA accession numbers for select cultures and specimens.

Ambrosia fungus	Associated ambrosia beetle	Specimen type	Isolate or specimen ID[1]	Location	Date collected	Collected by	ITS GenBank Accession No.
Ambrosiella							
Ambrosiella aff. *beaveri* NRbea1	*Xylosandrus germanus*	Culture from female (in *Lindera triloba*)	C4059	Aichi, Toyota, Inabu, Japan	July 2014	H. Kajimura	same as MG950182
	X. brevis	Culture from female (in *Lindera triloba*)	C4060	Aichi, Toyota, Inabu, Japan	July 2014	H. Kajimura	MG950181
	X. brevis	Culture from female (in *Lindera triloba*)	C4061 (CBS 142650)	Aichi, Toyota, Inabu, Japan	July 2015	H. Kajimura	MG950182
A. catenulata	*Anisandrus apicalis*	Culture from female	C3909	Morioka, Iwate Prefecture, Japan	Apr. 2015	H. Masuya	same as MG950184
	An. apicalis	Culture from female	C3910	Morioka, Iwate Prefecture, Japan	Apr. 2015	H. Masuya	same as MG950184
	An. apicalis	Culture from female	C3911	Morioka, Iwate Prefecture, Japan	Apr. 2015	H. Masuya	same as MG950184
	An. apicalis	Culture from female	C3912	Morioka, Iwate Prefecture, Japan	Apr. 2015	H. Masuya	same as MG950184
	An. apicalis	Culture from female	C3913 (CBS 142649)	Morioka, Iwate Prefecture, Japan	Apr. 2015	H. Masuya	MG950184
A. grosmanniae	*X. germanus*	Culture from female	C3901	Hachimantai, Iwate prefecture, Japan	June 2015	H. Masuya	same as KR611324
	X. germanus	Culture from female	C3902	Hachimantai, Iwate prefecture, Japan	June 2015	H. Masuya	same as KR611324
	X. germanus	Culture from female	C3903	Hachimantai, Iwate prefecture, Japan	June 2015	H. Masuya	same as KR611324
	X. germanus	Culture from female (in *Lindera triloba*)	C4058	Aichi, Toyota, Inabu, Japan	July 2010	H. Kajimura	MG950185
Ambrosiella aff. *grosmanniae* NRgro1	*Xylosandrus* aff. *germanus*	Culture from female	C3898	Iwate Prefecture, Morioka, Japan	Apr. 2015	H. Masuya	same as MG950186
	Xylosandrus aff. *germanus*	Culture from female	C3899 (CBS 142648)	Iwate Prefecture, Morioka, Japan	Apr. 2015	H. Masuya	MG950186
	Xylosandrus aff. *germanus*	Culture from female	C3900	Iwate Prefecture, Morioka, Japan	Apr. 2015	H. Masuya	same as MG950186
A. remansi	*Remansus mutabilis*	Propagules in mycangium of female in unidentified tree	M290 (BPI 910622) **HT**	Andasibe-Mantadia NP, Madagascar	May 2015	B. Jordal	KX342068
A. roeperi	*X. crassiusculus*	Culture from female (ethanol trap)	C3449	Fushan, Taiwan	July 2014	H.H. Shih	MG950187
	X. crassiusculus	Culture from female (in *Quercus crispula*)	C4062	Aichi, Toyota, Inabu, Japan	Sept. 2013	H. Kajimura	same as KF669871
Toshionella							
T. nipponensis	*S. shogun*	Culture from female (in unidentified tree)	C3904 (CBS 141492) **eHT**	Tazawako, Akita prefecture, Japan	July 2014	H. Masuya	KX342064
	S. shogun	Culture from female (in unidentified tree)	C3905	Tazawako, Akita prefecture, Japan	July 2014	H. Masuya	same as KX342064
	S. shogun	Culture from female (in unidentified tree)	C3906	Tazawako, Akita prefecture, Japan	July 2014	H. Masuya	same as KX342064
	S. shogun	Culture from female (in unidentified tree)	C4064	Hachimantai, Iwate prefecture, Japan	July 2014	H. Masuya	same as KX342064
T. taiwanensis	*S. pubescens*	Culture from female (ethanol trap)	C3687 (CBS 141494) **eHT**	Douna, Kaohsiung, Taiwan	Feb. 2014	H.H. Shih	KX342067
	S. pubescens	Culture from female (ethanol trap)	C3688	Jingdashan, Kaohsiung, Taiwan	Feb. 2014	H.H. Shih	same as KX342066
	S. mikado	Culture from female (ethanol trap)	C3448 (CBS 141495)	Lienhuachih, Taiwan	Aug. 2014	C. Wuest	same as KX342066
	S. mikado	Propagules in mycangium of female (ethanol trap)	M304	Lienhuachih, Taiwan	June 2014	H.H. Shih	same as KX342066
	S. mikado	Propagules in mycangium of female (in *Cinnamomum* sp.)	M305	Fushan, Taiwan	June 2014	H.H. Shih	same as KX342066
T. transmara	*S. shogun*	Culture from female (in unidentified tree)	C3908 (CBS 141493) **eHT**	Hachimantai, Iwate prefecture, Japan	June 2015	H. Masuya	KX342065
	S. tycon	Propagules in mycangium of female (ethanol trap)	sp1	Vladivostok, Russia	July 2008	B. Jordal	KX342066
	X. crassiusculus	Culture from female (in *Quercus crispula*)	C4063	Aichi, Toyota, Inabu, Japan	Sept. 2013	H. Kajimura	MG950183
Wolfgangiella							
W. franznegeri	*Scolytoplatypus fasciatus*	Propagules in mycangium of female in unidentified tree	sp2	Diepwalle Forest Station, Western Cape, South Africa	Nov. 2007	B. Jordal	same as MG950180
	S. fasciatus	Culture from female (ethanol trap)	C4325	Near Betty's Bay, Western Cape, South Africa	Jan. 2017	F. Roets	same as MG950180
	S. fasciatus	Culture from female (ethanol trap)	C4326	Near Betty's Bay, Western Cape, South Africa	Jan. 2017	F. Roets	same as MG950180
	S. fasciatus	Culture from female (ethanol trap)	C4327	Near Betty's Bay, Western Cape, South Africa	Jan. 2017	F. Roets	same as MG950180
	S. fasciatus	Culture from female (ethanol trap)	C4328 (CBS 144149) **eHT**	Near Betty's Bay, Western Cape, South Africa	Jan. 2017	F. Roets	MG950180
	S. fasciatus	Culture from female (ethanol trap)	C4329	Near Betty's Bay, Western Cape, South Africa	Jan. 2017	F. Roets	same as MG950180
	S. fasciatus	Culture from female (ethanol trap)	C4331	Near Betty's Bay, Western Cape, South Africa	Jan. 2017	F. Roets	same as MG950180
	S. rugosus	Ambrosia growth in *Ocotea* sp.	M288 (BPI 910640)	Andasibe-Mantadia NP, Madagascar	May 2015	B. Jordal	KX342063
W. madagascarensis	*S. permirus*	Ambrosia growth in unidentified tree	M286 (BPI 910641) **HT**	Ambohitantely FR, Madagascar	May 2015	B. Jordal	KX342062
	S. permirus	Ambrosia growth in unidentified tree	M399	Andasibe-Mantadia NP, Madagascar	May 2015	B. Jordal	same as KX342062
	S. permirus	Propagules in mycangium of female (ethanol trap)	sp3	Ranomafana NP, Madagascar	2012	B. Jordal	KX342061
Wolfgangiella sp.	*S. congonus*	Propagules in mycangium of female	M683	Cameroon	2017	B. Jordal	MH454339
	S. congonus	Propagules in mycangium of female	M685	Tanzania	2017	B. Jordal	MH454340

[1] Includes isolate or specimen numbers from the culture collection of T.C. Harrington, Iowa State University (C or M), Westerdijk Fungal Biodiversity Institute (CBS), and U.S. National Fungus Collections (BPI).
Holotype specimens indicated by **bold** 'HT'; ex-holotype cultures indicated by **bold** 'eHT'.

significant energy commitments by the beetles and are generally more specific in the fungi they carry (Harrington et al. 2014, Mayers et al. 2015, 2018, Skelton et al. 2019).

A variety of fungi are associated with ambrosia beetles (Harrington 2005, Skelton et al. 2018), but we define 'ambrosia fungi' in the strict sense (i.e., primary ambrosia fungi, after Batra 1985) as co-adapted symbionts that grow in ambrosia beetle mycangia, form a specially-adapted, dense layer of sporulation ('ambrosia') as food in the beetles' tunnels, and show no evidence of living independently (Francke-Grosmann 1963, 1967, Harrington et al. 2010, 2014, Mayers et al. 2015). With a recent exception in the wood-decay basidiomycete *Flavodon ambrosius* (Kasson et al. 2016, Simmons et al. 2016), only six genera in three orders of ascomycetous fungi meet these requirements: the polyphyletic *Raffaelea* s.lat. and monotypic *Afroraffaelea* in the family *Ophiostomataceae* (*Ophiostomatales*) (Harrington et al. 2010, Dreaden et al. 2014, Bateman et al. 2017); the *Fusarium* ambrosia clade (FAC) (*Hypocreales*) (Kasson et al. 2013, O'Donnel et al. 2015); and *Ambrosiella*, *Meredithiella*, and *Phialophoropsis* in the family *Ceratocystidaceae* (*Microscales*) (Mayers et al. 2015, 2018). Each lineage was most likely domesticated from ubiquitous, free-living companions, commensals, or contaminants in wood, as evidenced by their close relatives.

The large mycangia of ambrosia beetles have so far only been associated with the three ambrosial genera of *Ceratocystidaceae*, and each of the three fungal genera is exclusively associated with a different type of large mycangium (Mayers et al. 2015, 2018). The long-established genus *Ambrosiella* (Brader 1964, Von Arx & Hennebert 1965, Harrington et al. 2010) was restricted by Mayers et al. (2015) to a monophyletic group containing *Ambrosiella xylebori* and other species carried in the mesonotal pouch mycangia of ambrosia beetles in the *Xylosandrus* complex (tribe *Xyleborini*) (Skelton et al. 2019). *Ambrosiella* currently comprises nine species, all of which produce large aleurioconidia on branching monillioid conidiophores adapted for beetle grazing (Harrington et al. 2014, Mayers et al. 2015, 2017, Lin et al. 2017). *Meredithiella* accommodates three symbionts of *Corthylus* ambrosia beetles (tribe *Corthylini*), which have a winding procoxal tube (prothoracic coil) mycangium (Mayers et al. 2015, 2018). *Meredithiella* has alternately-branching conidiophores that produce aleurioconidia that are similar to those of *Ambrosiella* (Mayers et al. 2015, 2018). *Phialophoropsis* accommodates two named species and other putative species associated with the prothoracic pleural mycangia of *Trypodendron* (tribe *Xyloterini*) (Mayers et al. 2015, Lehenberger et al. 2019). *Phialophoropsis* is distinguished by the production of long chains of phialoconidia from deep-seated phialides and the absence of aleurioconidia (Mayers et al. 2015). All three genera were classically assumed to be strictly asexual, but the recent discovery of a sexual morph in *Ambrosiella cleistominuta* suggests cryptic sex may be common in ambrosia symbionts (Mayers et al. 2017).

Despite recent phylogenetic analyses of the *Ceratocystidaceae* (De Beer et al. 2014, 2017, Mayers et al. 2015, Nel et al. 2017) and an upswing in interest in the ambrosia symbiosis (Hulcr & Stelinski 2017), the phylogenetic relationships of the ambrosia beetle symbionts to the rest of the family remains poorly resolved (De Beer et al. 2014, Mayers et al. 2015, 2018). This is largely due to the difficulty of acquiring these fungi in pure culture (Francke-Grosmann 1963, 1967, Batra 1985) and the taxonomic gaps in the known ambrosia fungi in the *Ceratocystidaceae*. The *Scolytoplatypodini* comprise a fourth ambrosia beetle lineage with large mycangia, and their uncharacterized fungal symbionts might provide missing links in the unresolved phylogenetic and evolutionary relationships of *Ceratocystidaceae* ambrosia fungi. The tribe *Scolytoplatypodini* have large disk-shaped pronotal mycangia (Schedl 1962, Beaver & Gebhardt 2006, Li et al. 2019), and some species in Japan and Taiwan have been associated with *Ambrosiella*-like symbionts (Nakashima et al. 1987, 1992, Nakashima 1989, Kinuura et al. 1991, Beaver & Gebhardt 2006) that may be distinct from *Ambrosiella* s.str. (Lin 2016, Ito & Kajimura 2017). The ambrosia fungi of other Asian *Scolytoplatypodini* and of the other major lineages of the tribe in Africa and Madagascar (Jordal 2013) remain unstudied.

Though there is conflicting evidence for species-level specificity between ambrosia beetles with large mycangia and their fungal partners (Mayers et al. 2015, 2018, Lin et al. 2017, Skelton et al 2019), each large mycangium type has so far yielded a single, distinct ambrosial genus in the family *Ceratocystidaceae*. We expected that the large mycangia of tribe *Scolytoplatypodini* would yield a fourth ambrosial genus in the *Ceratocystidaceae*. Tribe *Scolytoplatypodini* is possibly the oldest ambrosia beetle lineage with large mycangia (Jordal 2013, Gohli et al. 2017, Pistone et al. 2018), and we hypothesize that the genera of ambrosia fungi in the *Ceratocystidaceae* were derived from a single ancestral domestication by tribe *Scolytoplatypodini* and that descendents of this ambrosial ancestor were horizontally transferred to other beetle tribes after they developed large mycangia. If this is the case, we expect that the crown age of each mycangium type will predate the crown age of its associated ambrosia fungi.

Our major aims were to

1. characterise and describe the fungal associations of the major lineages in tribe *Scolytoplatypodini* (Asian *Scolytoplatypus*, African *Scolytoplatypus*, and *Remansus*);
2. resolve the ambiguous evolutionary history for ambrosia symbiosis in the *Ceratocystidaceae* based on phylogeny, morphology, host associations, and divergence date estimates; and
3. resolve the taxonomy of the family *Ceratocystidaceae* with delineation of new genera and species.

MATERIALS AND METHODS

Specimen collection and fungal isolation

In addition to previous cultures and specimens (Mayers et al. 2015, 2017, 2018), new material was collected from galleries and adults of ambrosia beetles in tribes *Scolytoplatypodini* and *Xyleborini* (Table 1). Fungal cultures were isolated from beetles by surface-sterilising, dissecting, and directly plating portions of the prothorax containing mycangia on fungal culture media (Mayers et al. 2015, 2017, 2018). Not all isolation attempts were successful from galleries and beetles, often due to desiccation of the fungal material, but we were often able to extract DNA and identify the fungal symbionts by ITS-rDNA barcoding.

Microscopic observations

Dissected mycangia and fungal material scraped from gallery walls or the surface of pure cultures were mounted in lactophenol and cotton blue or lactic acid to be viewed with an Olympus BH-2 compound microscope (Mayers et al. 2017, 2018). Photographs were captured with a Leica DFC295 camera and Leica Application Suite V3.6 (Leica Camera Inc., Allendale, NJ). Contrast and brightness levels of some images were adjusted with Leica Application Suite or Adobe Photoshop CS6 (Adobe Systems Incorporated, San Jose, CA). Some images are composites of multiple photographs taken at different focus planes and combined with CombineZP (Hadley 2010). Some illustrations of mycangia are composites of multiple images taken at the same magnification and stitched together with the Photomerge function in Adobe Photoshop CS6.

Species descriptions

Isolates were grown on malt yeast extract agar (MYEA; 2 % malt extract, Difco Laboratories, Detroit, MI, USA; 0.2 % yeast extract, Difco; 1.5 % agar, Sigma-Aldrich, St. Louis, MO, USA) at room temperature. Agar plugs cut with a #1 cork borer (3 mm diam) were transferred from the leading margin of growth to three new MYEA plates, incubated at 25 °C for 7 d in the dark, and the diameter of the colonies measured. Colors are per Rayner (1970). Representative cultures were deposited in the Westerdijk Fungal Biodiversity Institute (CBS), and representative dried specimens were deposited in the U.S. National Fungus Collections (BPI).

DNA extraction, amplification, and sequencing

When working with small amounts of gallery growth, dissected mycangia, or whole beetles, DNA extractions generally used the PrepMan® Ultra kit (Applied Biosystems, Foster City, CA, USA), and extracts were concentrated when needed with Amicon® ultra-0.5 Centrifugal Filter Devices (EMD Millipore, Billerica, CA, USA). Extractions from pure cultures generally used the Promega Wizard® Genomic DNA Purification Kit (Promega, Madison, WI) or, when pigments inhibited PCR amplification, the E.Z.N.A. Fungal DNA Mini Kit (Omega Bio-Tek, Norcross, GA).

For routine species identification, amplification and sequencing of the nuclear rDNA ITS1-5.8S-ITS2 (internal transcribed spacer region, ITS barcode) (Schoch et al. 2012) used fungal primers ITS1F and ITS4 (Gardes & Bruns 1993, White et al. 1990). The *Ceratocystidaceae*-specific ITS primer sets Cerato-1F/ITSCer3.7R and ITSCer3.5/ITS4 (Mayers et al. 2015) were also used to obtain sequences from DNA extracts from galleries, mycangia, and whole beetles. All ITS amplification used the same PCR conditions (85 °C for 2 m; 95 °C for 95 s; 36 cycles of 58 °C for 1 m, 72 °C for 80 s, and 95 °C for 70 s; 52 °C for 1 m; 72 °C for 15 m; and 4 °C hold).

Six nuclear genes were sequenced for multi-locus phylogenetic analyses. For nuclear large subunit ribosomal DNA (28S rDNA), primers LR0R and LR5 were used for amplification with the same PCR conditions as the ITS barcode, and primers LR0R and LR3 were used for sequencing (Vilgalys & Hester 1990, Rehner & Samuels 1994). For nuclear small subunit ribosomal DNA (18S rDNA) amplification and sequencing, a combination of general primers (NS1, NS3, NS6, NS7, NS8, SR1R, and SR9R) were used (Elwood et al. 1985, Vilgalys & Hester 1990, White et al. 1990), as well as a new primer designed for ascomycetes ('NS4Asco', 5'-CTTCCGTCAATTTCTTTAAG-3', used in place of NS4) and two primers designed to specifically amplify fungal 18S rDNA from mycangia ('NS4Cer', 5'-CACTTTGATTTCTCGAAAG-3', used in place of NS4; and 'SR9RCer', 5'-GGCATCAGTATTCAGCTGTC-3', used in place of SR9R). All 18S rDNA PCR used the same PCR conditions (94 °C for 2 m; 36 cycles of 94 °C for 30 s, 52 °C for 30 s, and 72 °C for 1 m; 72 °C for 5 m; and 4 °C hold), but annealing temperature was lowered to 49 °C in some cases. For translation elongation factor 1-alpha (*tef*1-α), primers EFCF1 and EFCF6 were used for amplification with the PCR conditions of Oliveira et al. (2015), though we generally replaced EFCF1 with a new primer designed to avoid a problematic intron in many isolates ('EFCF1.5', 5'-GCYGAGCTCGGTAAGGGYTC-3'). Internal primers EFCF2 (Oliveira et al. 2015) and another new primer ('EFCer3', 5'-CARACHCGTGAGCAYGCTCT-3') were occasionally used for supplemental internal sequencing. Amplification and sequencing of beta-tubulin (*tub*) used the primers (Bt1a and Bt1b) and conditions of Glass & Donaldson (1995). Amplification and sequencing of the 60S ribosomal protein L1 (*rpl*1) and the DNA replication licensing factor *mcm*7 (minichromosome maintenance complex component 7) used the primers (60S-506F/60S-908R and Cer-MCM7F/Cer-MCM7R) and conditions of De Beer et al. (2014), but for some isolates the annealing temperature was reduced to 55 °C. Sequencing was performed by the Iowa State University DNA Sequencing Facility, and electropherograms of complementary and overlapping reads were examined, compared, and assembled using Sequence Navigator v. 1.0.1 or AutoAssembler v. 1.3.0 (Applied Biosystems, Foster City, California).

Molecular phylogeny

The ITS rDNA sequences of the *Ceratocystidaceae* have numerous indels that are ambiguously aligned, so for barcoding purposes, ITS sequences were manually aligned in two separate datasets: one for *Ambrosiella* and close relatives (TreeBASE URL: http://purl.org/phylo/treebase/phylows/study/TB2:S23518) and one for *Phialophoropsis* and close relatives (TreeBASE URL: http://purl.org/phylo/treebase/phylows/study/TB2:S23519). In addition to new ITS sequences (Table 1), alignments included ITS sequences newly generated from *Ceratocystis adiposa*, available from previous studies (Harrington et al. 2014, Mayers et al. 2015, 2017, 2018, Lin et al. 2017), obtained from selected *Phialophoropsis* isolates in another study (Mayers et al. unpubl.), or provided by the laboratory of J. Hulcr (University of Florida), as detailed in Table S1. A separate maximum parsimony tree was created from each of the two alignments with PAUP v. 4.0b10 (Swofford 2002) using heuristic searches with gaps treated as fifth character (which preserved the important diagnostic signals present in indels), starting trees obtained via stepwise addition, and the tree-bisection-reconnection branch-swapping algorithm. Using *C. adiposa* and *M. norrisii* as a monophyletic sister group to the ingroup, the *Ambrosiella* alignment had 552 characters, of which 135 were parsimony-informative, 43 were variable but parsimony-uninformative, and 374 were constant. The *Phialophoropsis* alignment used *Bretziella fagacearum* as outgroup with midpoint rooting, with 509 characters, of which 45 were parsimony-informative, 30 were variable but parsimony-uninformative, and 434 were constant. A representative tree was chosen from the trees produced from both alignments for illustration, and branch support values were generated for both trees via 1 000-replicate bootstrap maximum parsimony analysis in PAUP.

All multi-locus analyses used a manually-aligned, concatenated alignment (TreeBASE URL: http://purl.org/phylo/treebase/phylows/study/TB2:S22560) of 18S rDNA, *tef*1-α, 28S rDNA, *tub*, *mcm*7, and *rpl*1. Accession numbers for newly-generated sequences and those from previous studies (De Beer et al. 2014, Mayers et al. 2015, 2017, 2018, Lin et al. 2017) are listed in Table S2. Representatives of all major lineages in the *Ceratocystidaceae* were included (De Beer et al. 2014, 2017, Nel et al. 2017), but a close relative of the family, *Cornuvesica* (Marincowitz et al. 2015), was not included in analyses due to inadequate sequence data. Sequences also included those of a Michigan isolate of an unnamed *Microascales* sp. (C3547 = CBS 142647) we obtained from a gallery of the ship timber beetle, *Elateroides lugubris* (family *Lymexylidae*), which is not an ambrosia beetle. Sequences for the six genes were also extracted from genome assemblies available in the NCBI database (National Center for Biotechnology Information, Bethesda, Maryland): *Huntiella moniliformis* JMSH00000000 (Van der Nest et al. 2014), *Huntiella bhutanensis* MJMS00000000 (Wingfield et al. 2016b), and *Scedosporium boydii* NJFT00000000 (Duvaux et al. 2017). The resulting six-gene alignment had 5 276 characters. Introns were eliminated from *tef*1-α, *tub*, *mcm7*, and *rpl1*, as were ambiguously-aligned regions from 18S rDNA and 28S rDNA (618 characters total). The final alignment consisted of 4 658 characters, 3 347 of which were constant, 261 were variable but parsimony-uninformative, and 1 050 were parsimony-informative.

A Bayesian analysis of the six-gene alignment was performed with MrBayes v. 3.2.2 (Ronquist et al. 2012), with a single MCMC run with four chains (one cold, three heated) for 1 000 000 generations, which was sufficient to achieve an average standard deviation of split frequencies less than 0.002. Models and partitions were selected by PartitionFinder 2 (Lanfear et al. 2016) in 'mrbayes' mode, using 'aicc' (converted Aikaike Information Criterion) model selection and a greedy algorithm (Lanfear et al. 2012) and powered by PhyML (Guindon et al. 2010). As suggested by PartitionFinder 2, GTR+I+G was applied to the first partition (18S rDNA), fifth partition (28S rDNA and *tub* codon position 1), sixth partition (*rpl1* codon position 2 and *tub* codon position 2), seventh partition (*mcm7* codon position 1), tenth partition (*rpl1* codon position 1), and eleventh partition (*rpl1* codon position 3); GTR+G was applied to the third partition (*tef*1-α codon position 3 and *tub* codon position 3) and ninth partition (*mcm7* codon position 3); GTR+I was applied to the eighth partition (*mcm7* codon position 2); and F81+I+G was applied to the second partition (*tef*1-α codon position 2) and fourth partition (*tef*1-α codon position 1). A consensus tree was generated using the function 'sumt' with a burn-in value of 150 000 and visualized with FigTree v. 1.4.0. In addition to posterior probability values provided by MrBayes, additional branch support values were generated for the tree via 1 000-replicate bootstrap maximum likelihood analysis in RAxML (Mayers et al. 2018) and 1 000-replicate bootstrap parsimony analysis in PAUP.

The resulting Bayesian inference tree was annotated with symbols representing the production of necked perithecia (Nag Raj & Kendrick 1975, Upadhyay 1981, De Beer et al. 2014), fertile cleistothecia or immature spherical ascocarps (Mayers et al. 2015, 2017, 2018), and aleurioconidia, as reported in the literature or observed in our available cultures and specimens.

Divergence date estimates

For the primary analysis (Analysis A), a time-calibrated Bayesian tree with estimates of divergence dates was generated using BEAST v. 2.4.7 (Bouckaert et al. 2014) and an .xml file created in BEAUti 2 from the same six-gene alignment used to create the Bayesian inference tree of the *Ceratocystidaceae*. Most genera were pruned to two representative species, and the sequences from three additional outgroup taxa were extracted from genomes of *Aspergillus niger* ASM285v2 (Pel et al. 2007), *Sclerotinia sclerotiorum* AAGT01000000 (Amselem et al. 2011), and *Xylaria* sp. JS573 JWIU00000000 (Lee et al. unpubl. data). In the absence of fossils of *Ceratocystidaceae*, secondary calibrations were applied in uniform distributions (Schenk 2016) to the *Leotiomycetes-Sordariomycetes* crown (267–430 Ma) and the *Sordariomycetes* crown (207–339 Ma), defined as the 95 % highest posterior density (HPD) range from the 5-fossil-calibrated analysis of Beimforde et al. (2014). Site models were unlinked, and the tree and relaxed log normal clock were linked for all partitions. The birth-death model (Gernhard 2008) was used for the tree prior. Preliminary runs using the same models and partitions selected by PartitionFinder 2 for the MrBayes analysis were examined with Tracer 1.6 (Rambaut et al. 2014), but these gave unacceptably low effective sample size values (ESS below 100) for both the posterior and prior distributions. This appeared to be due to certain base substitution rates tending towards zero, which we interpreted as overparameterization (Surina et al. 2014). To mitigate this, the models for partitions 3, 6, 7, 9, 10, and 11 were relaxed from the GTR to the HKY model, which yielded acceptable ESS values. In the final analysis two separate MCMC runs of 25 000 000 generations were performed with pre-burn-ins of 150 000 and their output combined with LogCombiner 2.4.7. The combined output was analyzed with Tracer v. 1.6, resulting in all ESS values above 200 and convergence in the prior, likelihood, and posterior values. The tree files from both runs were combined and reduced to 10 000 trees with LogCombiner 2.4.7, then a maximum clade credibility tree was created and annotated with TreeAnnotator v. 2.4.7 with 15 % burn-in and median height nodes, which was visualized with FigTree v. 1.4.0.

A secondary analysis (Analysis B) using a 28S rDNA molecular clock was performed as a comparison to Analysis A for selected nodes, after the methods of Berbee & Taylor (2010). The highest pairwise distance (Kimura 2-parameter model) on each side of the node was used from the 28S rDNA dataset of 1 663 aligned characters. This pairwise distance was divided by two and multiplied by 100 to obtain percent base substitutions per lineage, which was multiplied by 100 Ma/1.25 %, considered to be a reasonable estimate for 28S substitution rate for the higher fungi (Berbee & Taylor 2010).

The estimated fungal divergence dates were compared to the origins of their associated mycangia using the crown dates estimated by Gohli et al. (2017) and Pistone et al. (2018). Specifically, the mesonotal pouch mycangium clade included the monophyletic *Xylosandrus* complex (Johnson et al. 2018, Skelton et al. 2019) (i.e., *Xyleborini* genera with mesonotal mycangia: *Anisandrus*, *Cnestus*, *Eccoptopterus*, *Hadrodemius*, and *Xylosandrus*); the prothoracic coil mycangium clade included *Corthylus* (subtribe *Corthylina*)*;* the prothoracic pleural mycangium clade included *Trypodendron* (tribe *Xyloterini*); and the pronotal disk mycangium clade included *Remansus* and *Scolytoplatypus* (tribe *Scolytoplatypodini*). Both Gohli et al. (2017) and Pistone et al. (2018) used four relevant fossils and BEAST to estimate divergence times for clades within the subfamily *Scolytinae*. Gohli et al. (2017) used 5 genes from 305 species, whereas Pistone et al. (2018) used 18 genes from 182 species. The Pistone et al. (2018) estimates were used for tribe *Scolytoplatypodini* and *Trypodendron* due to identical taxon coverage but far more gene data, and the Gohli et al. (2017) estimate was the only one available for *Corthylus*. For the *Xylosandrus* complex, which diverged early in tribe *Xyleborini* (Johnson et al. 2018) and should be only slightly younger than the tribe, the younger estimate by Pistone et al. (2018) of 14.3 Ma for the entire tribe *Xyleborini* was used. The older estimate of 22.5 Ma for the *Xylosandrus* complex by Gohli et al. (2017) is likely due to a combination of oversampling of *Xyleborini* taxa and a smaller number of genes, which resulted in inflated divergence estimates compared to other studies of the tribe (Jordal et al. 2000, Farrell et al. 2001, Jordal & Cognato 2012, Cognato et al. 2018, Pistone et al. 2018). Small discrepencies between the dates used in this study and those presented in Gohli et al. (2017) and Pistone et al. (2018) are due to our use of median node ages from raw data provided by the authors.

Ancestral state reconstruction

To infer the ancestral symbiotic state of nodes in the *Ceratocystidaceae*, FigTree v. 1.4.0 was first used to root the consensus tree produced by MrBayes to a single outgroup (*S. boydii*). Then, each species was coded as 'ambrosial' (0) or 'not ambrosial' (1), which included plant pathogens or putative saprophytes. Analysis was performed on the *S. boydii*-rooted tree with BayesTraits 2.0.2 in 'MultiState' mode with internal nodes defined with MRCA, and involved 10 000 000 Reverse Jump MCMC iterations, exponential priors with mean 30, and burn-in of 100 000 generations. The resulting ancestral probabilities were visualized as pie graphs in TreeGraph v. 2.14 by applying the log output from BayesTraits to the *S. boydii*-rooted Bayesian tree using 'Import BayesTraits data…' in TreeGraph. Selected pie graphs were transferred to the BEAST time-calibrated tree.

RESULTS

Fungus-beetle associations

We successfully identified putative species of *Ceratocystidaceae* from 10 species of *Scolytoplatypodini* representing the three recognised lineages of the tribe (Jordal 2013), including four species from the African/Malagasy lineage of *Scolytoplatypus* (*S. congonus*, *S. fasciatus*, *S. permirus*, and *S. rugosus*), seven species from the Asian lineage of *Scolytoplatypus* (*S. daimio*, *S. eutomoides*, *S. mikado*, *S. pubescens*, *S. raja*, *S. shogun*, and *S. tycon*), and a species of *Remansus* (*R. mutabilis*) (Table 1). Three different genera of *Ceratocystidaceae* appeared to be associated with the *Scolytoplatypodini*, and one of the fungus species was found to have a sexual morph. We also generated sequences from *Ambrosiella* symbionts of five Asian *Xyleborini* species (*Anisandrus apicalis*, *Xylosandrus brevis*, *X. crassiusculus*, *X. germanus*, and *X.* aff. *germanus*). Several *Ceratocystidaceae* species were associated with more than one beetle species, as reported previously (Lin et al. 2017, Mayers et al. 2018), but for the first time, individual ambrosia beetle species (in Asian *Scolytoplatypus*) were associated with more than one species of *Ceratocystidaceae*.

African and Malagasy *Scolytoplatypus*

Galleries of *S. permirus* from two different locations in Madagascar (Table 1) had thick, homogeneous, white-grey ambrosia growth, and the larval cradles were sealed from the main tunnels by frass and fragmented mycelium. The material was desiccated, and isolation attempts from the galleries and the females inside were unsuccessful. The DNA extracted from the ambrosia growth in both galleries yielded the same ITS sequence, which grouped within the *Ceratocystidaceae* and was most similar to but distinct from *Phialophoropsis* (Fig. 1). Phialidic conidiophores expected of *Phialophoropsis* were not seen, but the ambrosia growth contained monilioid branches of disarticulating, irregular to globose, thallic-arthric propagules (Fig. 2n–r). A homogeneous mass of thallic-arthric fungal propagules that were solitary or in short chains (Fig. 2t) were found in the mycangium of a *S. permirus* female from a third location in Madagascar (Table 1). The DNA from this mycangial spore mass yielded an ITS sequence nearly identical (Fig. 1) to that obtained from the two galleries of *S. permirus* (but with a repeated 'TC' in the first variable region of ITS1).

A gallery of *S. rugosus* in Madagascar had ambrosia growth that appeared similar to that in galleries of *S. permirus*, and DNA extracted from the *S. rugosus* gallery yielded an ITS sequence nearly identical to sequences of the fungus associated with *S. permirus* (Fig. 1), though lacking a repeated 'CC' in the first variable region of ITS1. Isolations from the desiccated gallery and the single female inside were not successful. Conidiophores in the gallery of *S. rugosus* (Fig. 2g) were similar to those in galleries of *S. permirus*, but the *S. rugosus* galleries had spherical ascomata embedded in the homogenous mat of ambrosia growth. The ascomata lacked necks or ostioles and released large, banana-shaped ascospores when crushed (Fig. 2d).

DNA extracted from the mycangium contents of a South African *S. fasciatus* female preserved in ethanol (Table 1) yielded an ITS sequence identical to that recovered from the Malagasy *S. rugosus* gallery (Fig. 1). Isolations from the mycangia of six fresh South African *S. fasciatus* females collected using ethanol-baited traps yielded isolates of a green-grey, slow-growing fungus (Fig. 2a), and the ITS sequences derived from these cultures were identical to the one obtained from the preserved *S. fasciatus* specimen (Fig. 1). The six cultures produced branching, disarticulating, thallic-arthric propagules (Fig. 2h–m) similar to those observed in the *S. rugosus* galleries, and the six cultures also produced spherical, immature ascomata. In two of the isolates (C4325 and C4328), the ascomata matured and produced large, banana-shaped ascospores (Fig. 2c, e) identical to those produced by the ascomata in the *S. rugosus* gallery. Single ascospores transferred from isolate C4328 to MYEA from fertile ascomata using a sterile needle (Mayers et al. 2017) germinated from both ends of the spores (Fig. 2f). The resulting colonies were similar in appearance to the parent culture and yielded identical ITS sequences, but the colonies did not produce ascomata and appeared debilitated in that they produced less surface growth, had a slower growth rate, and attained smaller maximum colony diameters.

ITS sequences were obtained from the mycangia of two female *S. congonus* caught in 2017 in Cameroon (MH454339

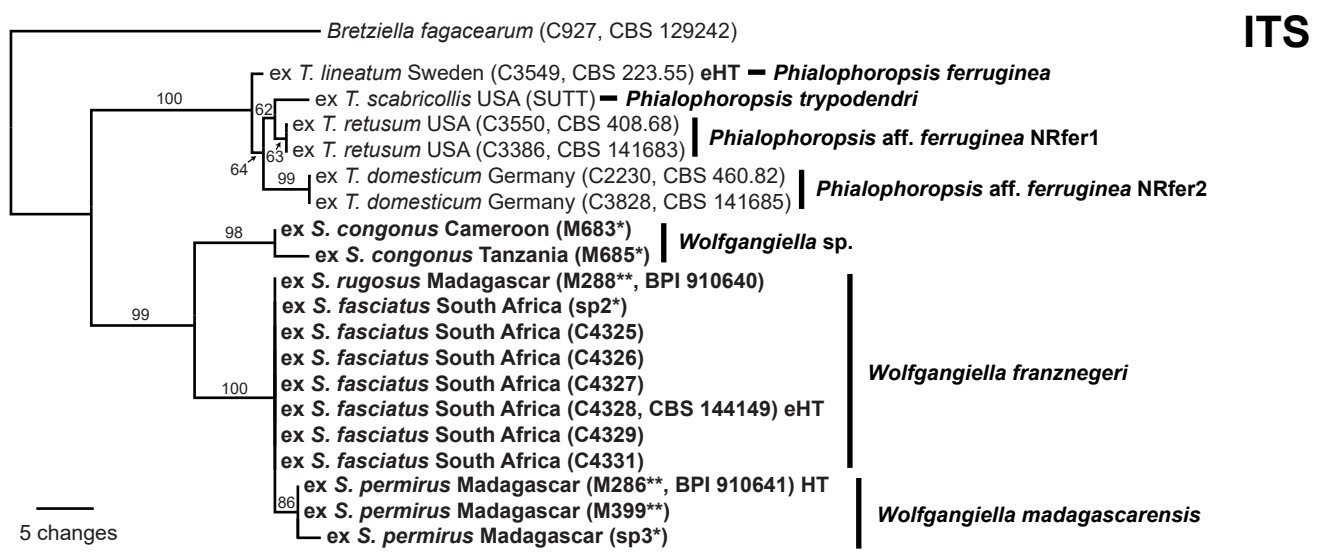

Fig. 1 The single most parsimonious tree produced from analysis of ITS rDNA sequences of cultures and specimens of *Phialophoropsis* and close relatives from the collections at Iowa State University (C or M), Westerdijk Fungal Biodiversity Institute (CBS), or U.S. National Fungus Collections (BPI). Sequences in **bold** are new. Single asterisk (*) indicates sequence obtained from DNA extracted from whole beetle or mycangial spore mass; double asterisks (**) indicate sequence from DNA extracted from gallery growth. Country of origin of the beetle, gallery, or culture is indicated. Bootstrap support values (> 50 %) from 1 000-replicate maximum parsimony analysis are indicated on branch labels. *Bretziella fagacearum* was used as an outgroup. CI = 0.9438. An 'e' indicates an ex-type culture; HT = holotype; IT = isotype; PT = paratype. — Scale bar = 5 changes (bp).

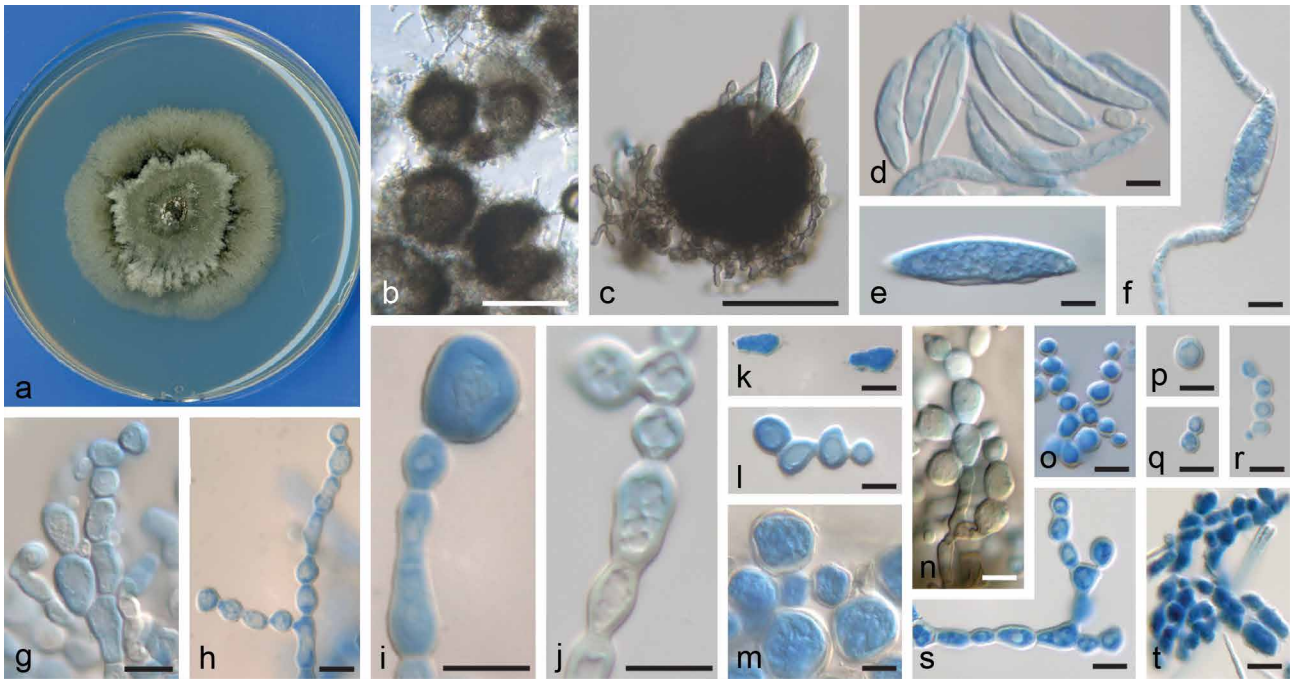

Fig. 2 *Wolfgangiella franznegeri* (a–m) and *W. madagascarensis* (n–t). a. Culture at 15 d on MYEA; b. ascomata; c. ascospores emerging from ascocarp; d–e. ascospores; f. germinating ascospore; g–j. conidiophores; k–l. detached thallic-arthric conidia; m. larger, thick-walled propagules in culture; n–s. conidiophores and detached thallic-arthric conidia; t. propagules in mycangium of *S. permirus* (a, c, e–f, h, j–k. ex-holotype isolate CBS 144149 from *S. fasciatus*; b. isolate C4325 from *S. fasciatus*; d, g. from gallery BPI 910640 of *S. rugosus*; i, l. isolate C4329 from *S. fasciatus*; m. isolate C4331 from *S. fasciatus*; n–s. holotype BPI 910641 from gallery of *S. permirus*; t. mycangium mass sp3 from *S. permirus*; all photos (except a) by Nomarski interference microscopy of material stained with cotton blue; a imaged with Epson 10000XL). — Scale bars = 10 µm.

from DNA extract M683) and Tanzania (MH454340 from DNA extract M685). The two sequences were similar to each other, but the Tanzania sequence has an extra repeated 'C' in ITS1, an A/G transition in ITS1, and a G/A transition in ITS2. Phylogenetic divergence was also observed between specimens of *S. congonus* from Cameroon and Tanzania (Jordal 2018). The fungal ITS sequences from the *S. congonus* specimens formed a distinct sister group to the ITS sequences from other African *Scolytoplatypus* (Fig. 1), mirroring the phylogenetic relationship of *S. congonus* and the other African species of *Scolytoplatypus* (Jordal 2018).

Asian *Scolytoplatypus*

Fungal isolates from the mycangia of *Scolytoplatypus* spp. in Japan and Taiwan (Table 1) had ITS sequences that were unique within the *Ceratocystidaceae* but were most similar to those of *Ambrosiella* (Fig. 3). Five Japanese *S. shogun* females yielded green-grey, slow-growing cultures (Fig. 4a, g, q) with an identical ITS sequence. All five isolates produced terminal, globose, thick-walled aleurioconidia (Fig. 4b–e) that were much larger than those observed in *Ambrosiella* (Mayers et al. 2015, 2017, Lin et al. 2017). The individual cells of the branching conidiophores occasionally became globose and thick-walled (Fig. 4c) and were difficult to differentiate from aleurioconidia.

A sixth isolate from *S. shogun* (C3908) had conidiophores and branching, disarticulating, thallic-arthric propagules (Fig. 4h–m), similar to those of the other *S. shogun* isolates, but C3908 had an atypical colony morphology (Fig. 4g) and a different ITS sequence. The DNA extracted from the mycangium of a Russian *S. tycon* (Table 1) yielded an ITS sequence that differed from C3908 at only one base position. Propagules in the *S. tycon* mycangium appeared to be thallic-arthric propagules (Fig. 4o–p), and in contrast to the propagules observed in mycangia of the Malagasy/African *Scolytoplatypus* spp., the propagules in the *S. tycon* mycangium appeared to sometimes branch, as illustrated in mycangia of *S. shogun* (Nakashima et al. 1987). Two *S. pubescens* females collected from different locations in Taiwan (Table 1) yielded isolates of a dark, olive-green fungus (Fig. 4q) with an ITS sequence that was most similar to those obtained from *S. shogun* and *S. tycon* (Fig. 3). Chains of aleurioconidia that formed in culture were generally longer and the conidiophores less branched compared to those in *S. shogun* isolates (Fig. 4r–v), and the *S. pubescens* isolates produced more aerial hyphae and unique vertical hyphae with branching, dark-brown chlamydospores (Fig. 4x–y). The DNA extracted from the mycangia of two *S. mikado* females and one isolate from a third Taiwanese *S. mikado* female yielded ITS sequences identical to that of the isolates from *S. pubescens* (Fig. 3). Isolate C3448 from *S. mikado* initially had a colony morphology similar to that of *S. pubescens* isolates, but C3448 later differentiated into a slower-growing form with a reddish tint. Propagules in the mycangia of *S. mikado* were single or chained, sometimes-branching and thallic-arthric (Fig. 4z).

Cultures isolated in 2002 from *S. daimio*, *S. mikado*, *S. shogun*, and *S. tycon* in Japan (Table 1) were lost, but partial to full ITS sequences were obtained in 2002 and compared to more recent sequences. The ITS sequences of the *S. daimio*, *S. mikado*, and *S. shogun* cultures grouped with sequences obtained from the new isolates from *S. shogun* (Fig. 3). The sequences from *S. tycon* isolates grouped more closely with those from the atypical *S. shogun* isolate C3908 and the *S. tycon* mycangium (Fig. 3). Small one- or two-bp differences among the 2002 ITS sequences may be due to ambiguities or errors encountered with older sequencing technology.

An ITS sequence provided by J. Skelton (U. Florida) from a spore mass oozing from the mycangium of a female *S. eutomoides* caught in Mu village, Chimbu Province, Papua New Guinea by J. Hulcr (U. Florida) was similar to the sequences of the Taiwan *Scolytoplatypus* spp., differing only in a 2-bp deletion in the variable region of ITS1 (Fig. 3). Two ITS sequences provided by You Li (U. Florida) from cultures isolated from the mycangia of two female *S. raja* caught in flight in mainland China (Guiyang, Guizhou, 2015 and Shiwandashan, Guangxi, 2018) were identical to the sequences obtained from *S. pubescens* and *S. mikado* in Taiwan (Fig. 3).

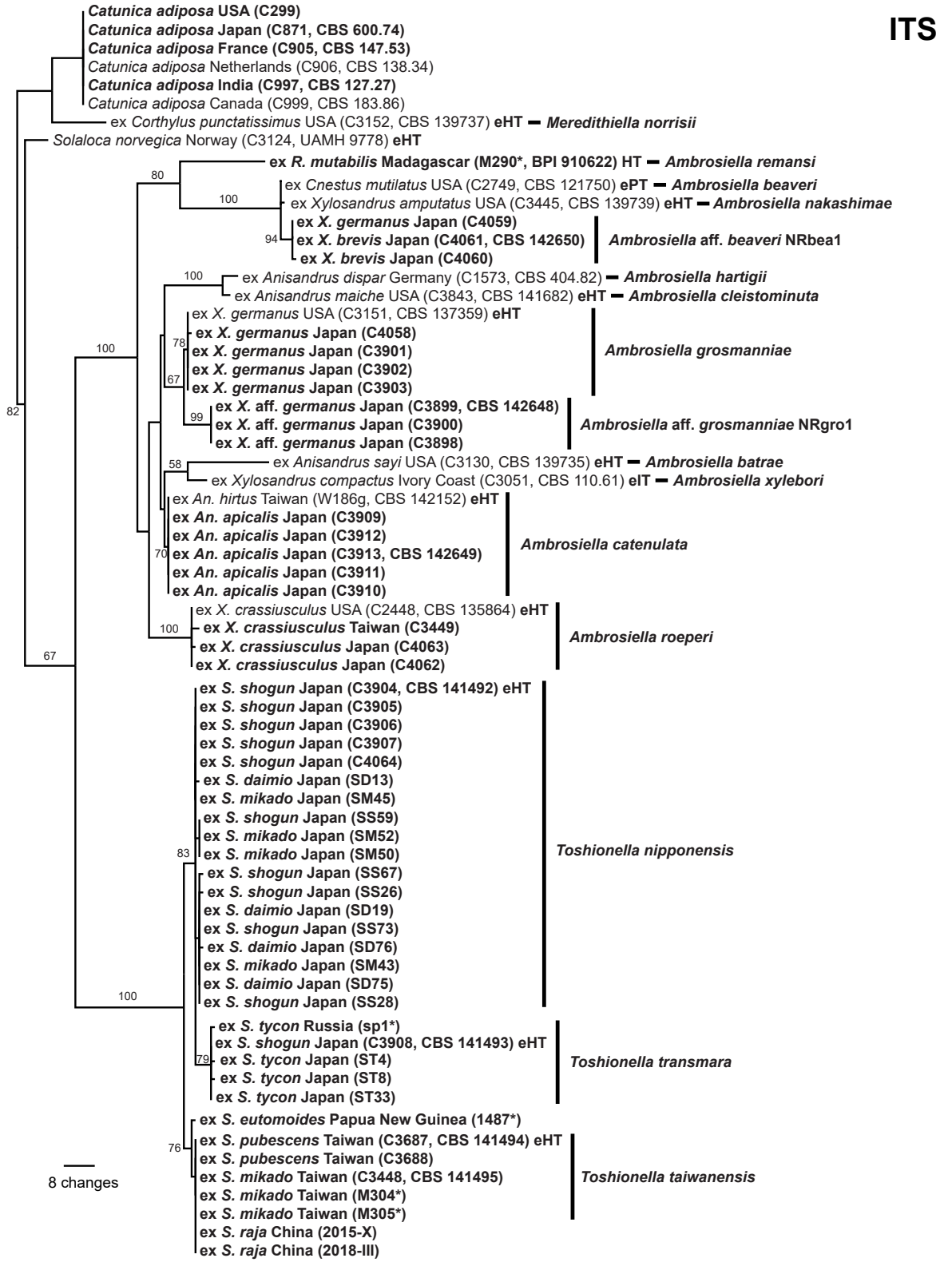

Fig. 3 One of 12 most parsimonious trees produced from analysis of ITS rDNA sequences of cultures and specimens of *Ambrosiella* and close relatives from the collections at Iowa State University (C or M), Westerdijk Fungal Biodiversity Institute (CBS), U.S. National Fungus Collections (BPI), the UAMH Centre for Global Microfungal Biodiversity (UAMH), or other collections. Sequences in **bold** are new. Single asterisk (*) indicates sequence obtained from DNA extracted from whole beetle or mycangial spore mass; double asterisks (**) from DNA extracted from gallery growth. Country of origin of the beetle, gallery, or culture is indicated. Bootstrap support values > 50 % indicated on branches. *Catunica adiposa* and *Meredithiella norrisii* were used as outgroups. CI = 0.7823. An 'e' indicates an ex-type culture; HT = holotype; IT = isotype; PT = paratype. — Scale bar = 8 changes (bp).

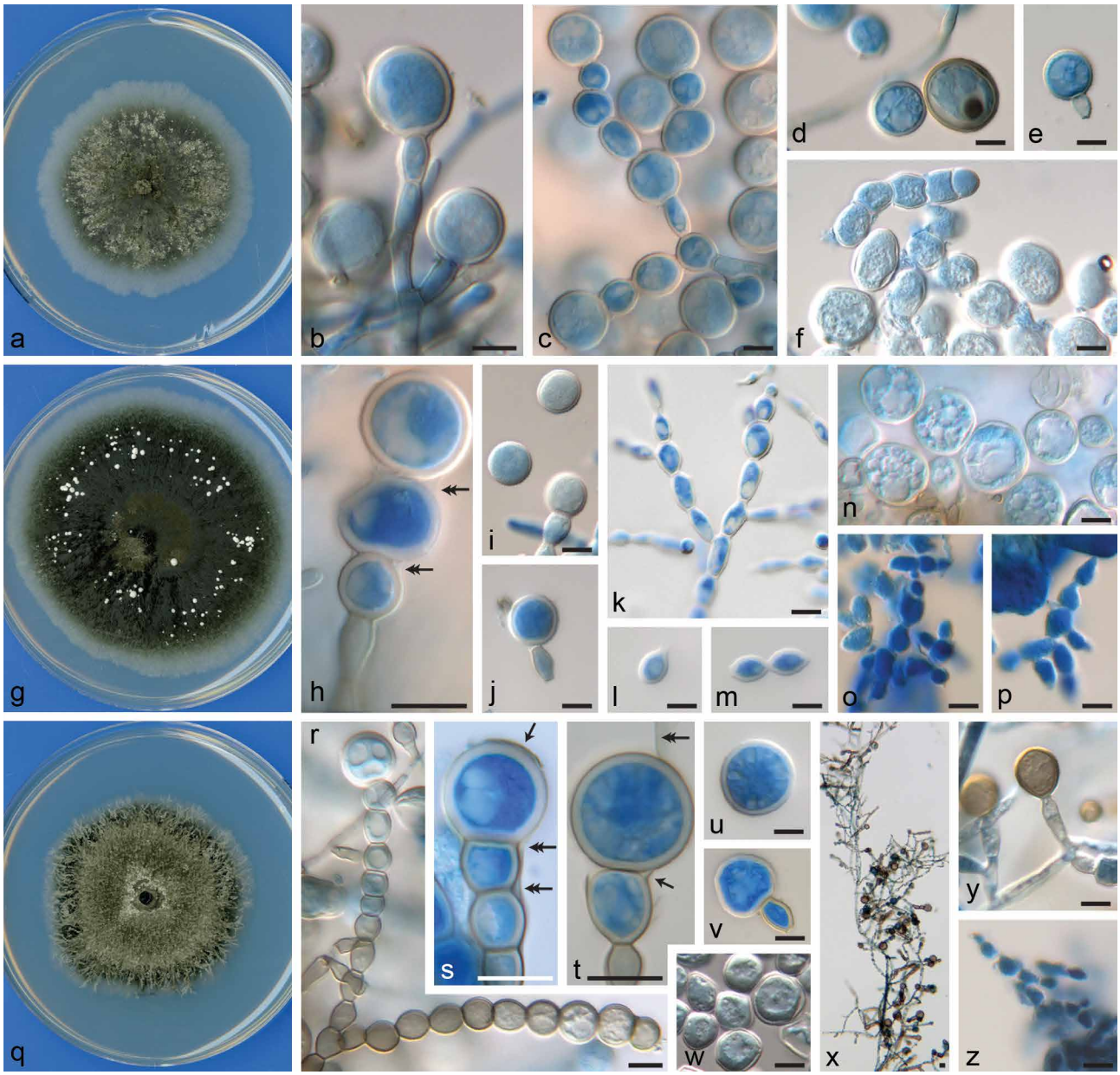

Fig. 4 *Toshionella nipponensis* (a–f), *T. transmara* (g–p), and *T. taiwanensis* (q–z). a, g, q. Culture morphology at 8.5 d on MYEA; b. conidiophores bearing aleurioconidia; c. conidiophore with globose, thick-walled cells; d. detached, single aleurioconidia; e. detached aleurioconidium with penultimate conidiophore cell attached; f. globose, thick-walled propagules forming wet mounds in culture; h. conidiophore bearing chain of aleurioconidia, with arrows indicating membranous sheath; i. detached solitary aleurioconidia; j. detached aleurioconidium with penultimate conidiophore cell attached; k. branched chains of disarticulating thallic-arthric conidia; l–m. detached thallic-athric conidia; n. globose, thick-walled propagules forming wet mounds in culture; o–p. propagules in mycangia of *Scolytoplatypus tycon*; r. long, branched conidiophore bearing aleurioconidia; s. young conidiophore with terminal aleurioconidium subtended by developing aleurioconidia, with single arrow indicating remnant of conidiogenous cell and double arrows indicating membranous sheath; t. aleurioconidium breaking free of conidiophore, with single arrow indicating collarette and double arrow indicating sloughing membranous sheath; u. solitary aleurioconidium; v. aleurioconidium with penultimate conidiophore cell attached; w. globose, thick-walled propagules forming wet mounds in culture; x. vertical hyphal tower bearing pigmented chlamydospores; y. pigmented chlamydospores; z. propagules in mycangium of *S. mikado* (a–f. ex-holotype isolate CBS 141492 from *S. shogun*; g–n. ex-holotype isolate CBS 141493 from *S. shogun*; o–p. mycangium mass sp1 from *S. tycon*; q–y. ex-holotype isolate CBS 141494 from *S. pubescens*; z. mycangium mass M304 from *S. mikado*; all photos (except a, g, q) by Nomarski interference microscopy of material stained with cotton blue; a, g, q imaged with Epson 10000XL). — Scale bars = 10 µm.

Remansus

Galleries of *R. mutabilis* collected in Madagascar (Table 1) appeared to be recently-initiated and devoid of ambrosia growth. The DNA extracted from the mycangium contents of a female taken from one of the galleries yielded an ITS sequence that closely matched sequences of *Ambrosiella* (Fig. 3). This mycangium was full of arthric-thallic propagules that were solitary or in short, linear chains (Fig. 5c–d) and were very similar to mycangium propagules of *Ambrosiella* (Harrington et al. 2014, Mayers et al. 2015, 2017). Isolations were unsuccessful from the desiccated galleries and from the mycangia of two other females.

Asian *Xyleborini* beetles

Isolations were made from several *Xyleborini* species in the *Xylosandrus* complex that were sympatric with the studied Asian *Scolytoplatypus* species. All of these *Xyleborini* had *Ambrosiella* symbionts, as expected (Mayers et al. 2015, 2017, Lin et al. 2017, Skelton et al. 2019) (Fig. 3). Three Japanese females identified as *Xylosandrus* aff. *germanus* yielded isolates of an undescribed species (*Ambrosiella* aff. *grosmanniae* NRgro1), which was morphologically distinct from *A. grosmanniae* and may coincide with cryptic diversity in *X. germanus* and its *A. grosmanniae* symbionts (Ito & Kajimura 2017). Two Japanese *X. brevis* and one Japanese *X. germanus* yielded isolates

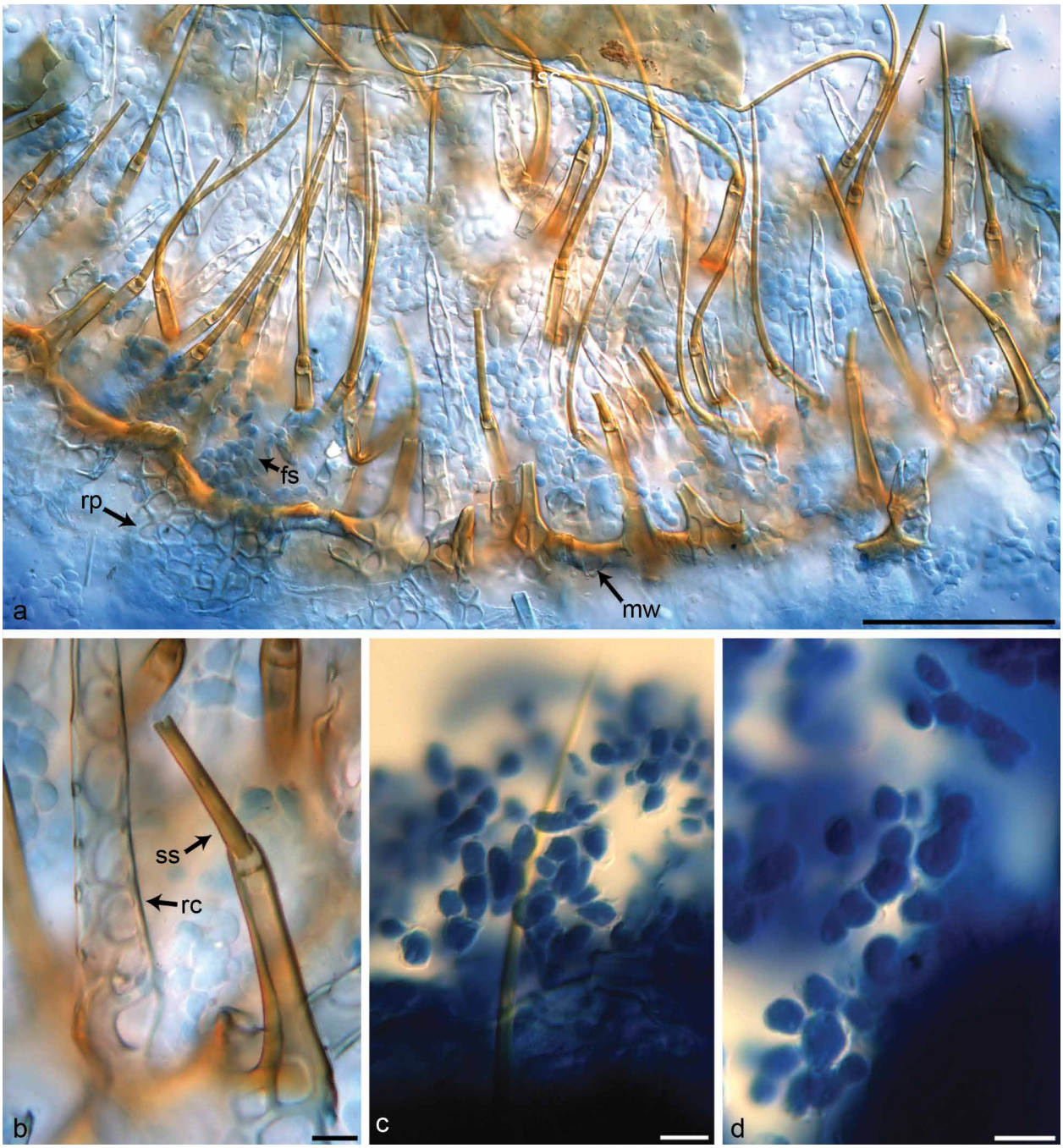

Fig. 5 Mycangium of *Remansus mutabilis* and mycangium propagules of *Ambrosiella remansi*. a. Cross-section of pronotal disk mycangium showing mycangium wall (mw), reticulated pouches (rp), and fungal spores (fs); b. detail of mycangium wall, showing socketed seta (ss) on hollow cylindrical pedestal and reticulated cone (rc); c. propagules of *A. remansi* surrounding seta; d. propagules of *A. remansi* (all photos by Nomarski interference microscopy of BPI 910622, stained with cotton blue). — Scale bars: a = 100 µm; b–d = 10 µm.

of what may be another undescribed species (*Ambrosiella* aff. *beaveri* NRbea1) in the *A. beaveri* complex (Fig. 3). Five Japanese *Anisandrus apicalis* yielded isolates of *Ambrosiella catenulata* (Fig. 3), the first report from this beetle species (Lin et al. 2017).

Prior to the discovery of the sexual morph of the *S. fasciatus* symbiont, *A. cleistominuta* was the only ambrosia beetle symbiont known to produce mature ascocarps (Mayers et al. 2017). As a morphological comparison, we sought ascomata of the type species, *A. xylebori*, the symbiont of *Xylosandrus compactus*, because galleries of this twig borer are easily collected from the dead branch tips on living trees (Greco & Wright 2015). We collected 87 dead twigs with small gallery entrance holes on various living hosts in Mississippi and Louisiana, USA in June and July 2016. Many galleries were abandoned or contained only adult beetles and sparse ambrosia growth, but 25 galleries had healthy ambrosia growth that could be confirmed to be *A. xylebori* by morphology, direct ITS barcoding of gallery scrapings, and/or isolation of pure cultures, including CBS 144147. Twelve of the galleries with healthy ambrosia growth had neckless ascomata embedded in the ambrosia layer (Fig. 6a) that appeared very similar to the ascomata of *A. cleistominuta* (Mayers et al. 2017). Two of the ascomata were plated onto MEA and produced cultures of *A. xylebori*, but these cultures produced no ascomata. Some of the gallery ascomata contained ascospores (Fig. 6b–d) nearly identical to those of *A. cleistominuta* and similar in size to those of the perithecia-forming *C. adiposa* (Fig. 6e) and *C. norvegica* (Fig. 6f). In comparison to the ascospores of *Ambrosiella*, or any other *Ceratocystidaceae*, the ascospores of the *S. fasciatus* isolates are dramatically larger (Fig. 6g).

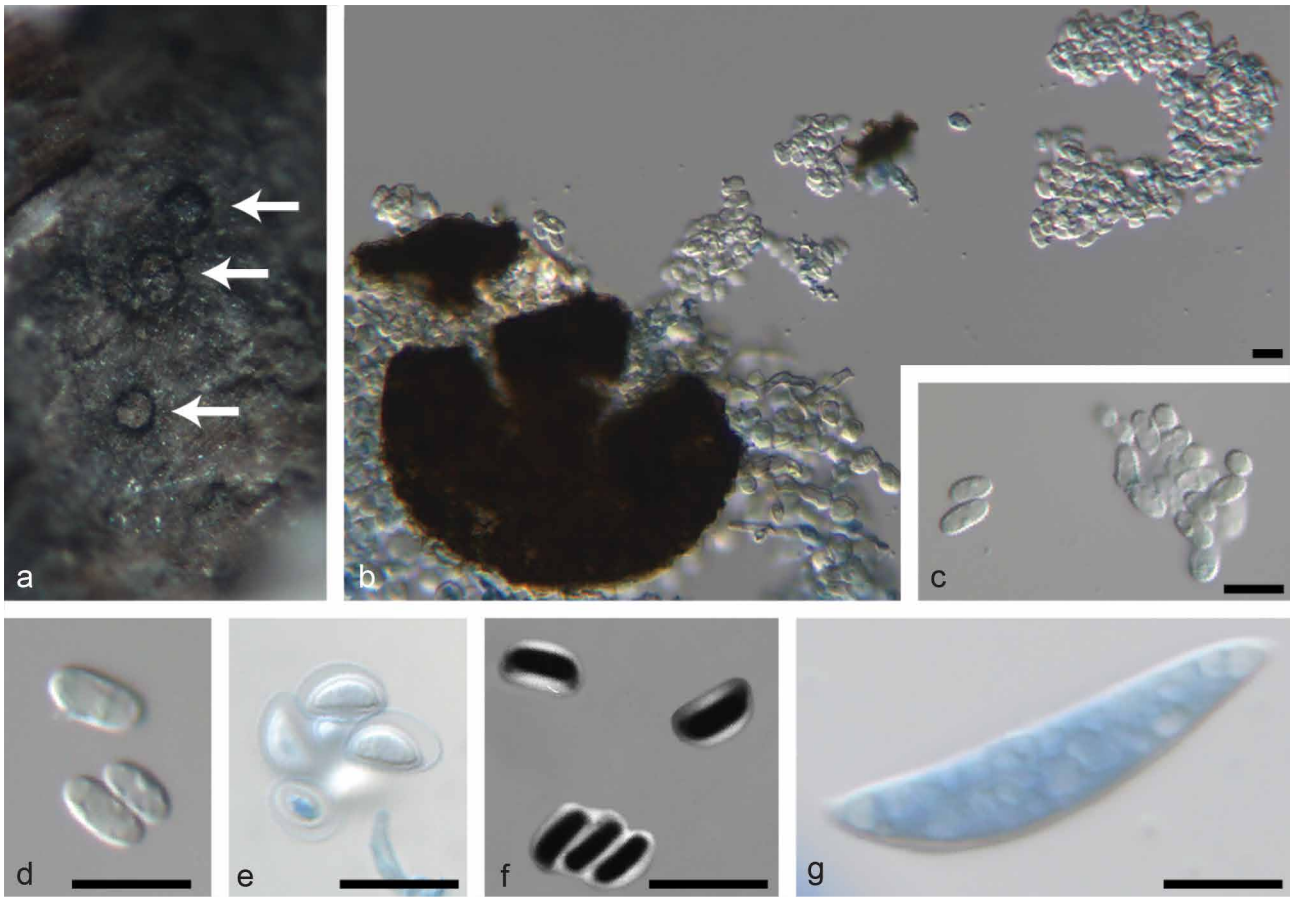

Fig. 6 Sexual morph of *Ambrosiella xylebori* (a–d), *Catunica adiposa* (e), *Solaloca norvegica* (f), and *Wolfgangiella franznegeri* (g). a. Grazed-open ascomata in gallery of *Xylosandrus compactus*; b. mass of ascospores ejected from crushed ascocarp; c–g. ascospores (all photos (except a) by Nomarski interference microscopy of material stained with cotton blue; a. imaged with stereo microscope). — Scale bars = 10 µm.

Scolytoplatypodini mycangia

Consistent with Schedl's (1962) illustrations, all observed mycangia of *Scolytoplatypodini* were disk-shaped cavities just under the cuticle on the dorsal side of the pronotum that emptied through a central, circular cuticular pore. Waxy masses of fungal propagules in an unidentified matrix generally plugged the pores and oozed out when pressure was applied to the dissected mycangium. As also seen in Schedl's illustrations, the interior of the *Scolytoplatypus* mycangia were lined with long setae that led towards the pore and presumably helped guide fungal propagules to exit. The morphology of these internal setae differed substantially between African and Asian *Scolytoplatypus* species. The setae of African *Scolytoplatypus* species (*S. congonus*, *S. fasciatus*, *S. permirus*, and *S. rugosus*) were of two types: shorter, thinner setae that grew directly from the sclerotized plates of the mycangium wall (Schedl's 'unechte Haare' or 'false hairs'), and longer, thicker setae that grew from short, cone-shaped sockets on the mycangium wall (Schedl's 'echte Haare' or 'true hairs'), as illustrated in the African species *S. acuminatus* (Schedl 1962). In contrast, the mycangia of Asian *Scolytoplatypus* species (*S. mikado*, *S. pubescens*, and *S. tycon*) had only one type of setae, which were socketed on the apexes of tall reticulated cones that were extensions of the reticulated network of the mycangium wall. This is a new description for mycangia of *S. pubescens*, and the setae match previous illustrations of the setae of *S. blandfordi*, *S. daimio*, *S. mikado*, *S. raja*, *S. shogun*, and *S. tycon* (Berger & Cholodkovsky 1916, Schedl 1962, Nakashima et al. 1987, Beaver & Gebhardt 2006, Li et al. 2019).

Mycangia of the rare and recently-described (Jordal 2013) genus *Remansus* had not been illustrated previously. The mycangia of female *R. mutabilis* collected in Madagascar were pronotal disks similar to those of *Scolytoplatypus*. However, the interior setae of the *Remansus* mycangium were of only one type, which were socketed on the apexes of tall, hollow, elongated, non-reticulated, cylindrical, and pigmented pedestals (Fig. 5a–b). Interspersed with these pedestals were tall reticulated cones (Fig. 5b) that did not support terminal setae but were otherwise similar to the cones supporting the interior setae of Asian *Scolytoplatypus*. The mycangium wall of *R. mutabilis* was composed of a large, reticulated network, between which hung more finely-reticulated, semi-spherical pouches (Fig. 5a). This reticulated network was more similar to the reticulated mycangium walls of Asian *Scolytoplatypus* than the sclerotized plates of African *Scolytoplatypus* (Schedl 1962). Both the setal pedestals and reticulated cones of *R. mutabilis* appeared to be contiguous with this reticulated network. Fungal propagules were found throughout the mycangium lumen as well as in the semi-spherical pouches (Fig. 5a).

Phylogenetic analyses

The recovered symbionts of the three *Scolytoplatypodini* lineages were members of the *Ceratocystidaceae*, but they did not form a monophyletic group. The ITS sequences of African *Scolytoplatypus* symbionts were most similar to *Phialophoropsis*. Parsimony analysis of the *Phialophoropsis*-affiliated alignment produced one tree (Fig. 1). The African *Scolytoplatypus* symbionts formed a distinct sister group to *Phialophoropsis*, with strong bootstrap support (Fig. 1). The ITS sequences of the mycangial symbionts of Asian *Scolytoplatypus* and *R. mutabilis* were more similar to *Ambrosiella*, and parsimony analysis of the *Ambrosiella*-affiliated alignment produced 84 trees (including Fig. 3) that differed only in the topology of the Japanese *Scolytoplatypus* symbionts that were sequenced in 2002. The

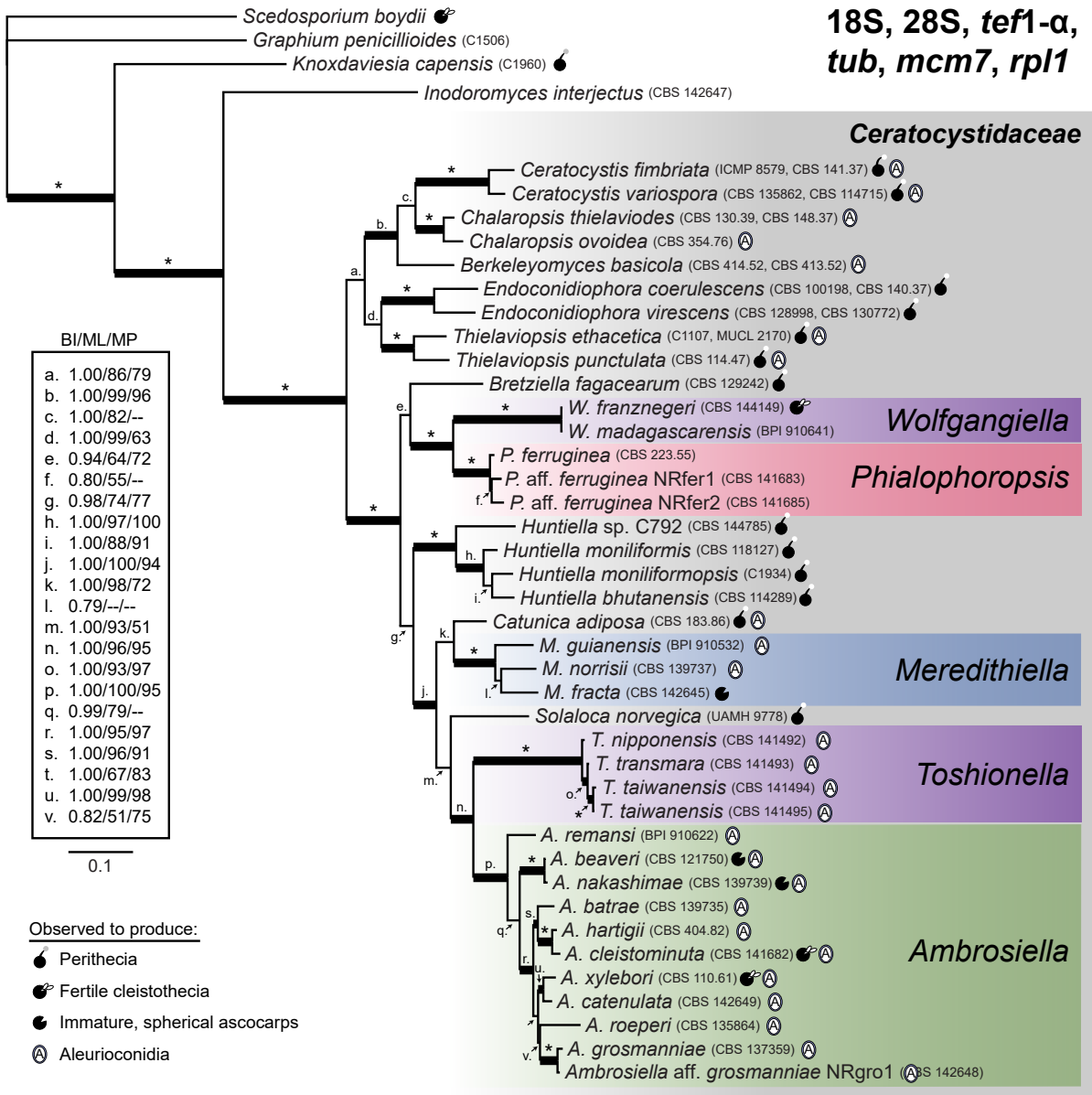

Fig. 7 Phylogenetic tree from Bayesian analysis of a six-gene dataset (18S rDNA, 28S rDNA, *tef*1-α, *tub*, *mcm7*, and *rpl1*) of ambrosia fungi and other representatives of the *Microascales* from the Iowa State University collection (C or M), Westerdijk Fungal Biodiversity Institute (CBS), U.S. National Fungus Collections (BPI), the Belgian Co-ordinated Collections of Micro-organisms (MUCL), the International Collection of Microorganisms from Plants (ICMP), or the UAMH Centre for Global Microfungal Biodiversity (UAMH). The family *Ceratocystidaceae* is indicated by a grey-shaded rectangle and the five ambrosia fungus genera are indicated by coloured rectangles. Symbols to the right of each taxon represent presence of sexual sporocarps or aleurioconidia. Posterior probabilities from Bayesian inference (BI), bootstrap support values from 1 000-replicate maximum likelihood analysis in RAxML (ML), and bootstrap support values from 1 000-replicate maximum parsimony analysis in PAUP (MP) are indicated in box at left margin with lowercase letters indicating the associated branch. Branches with BI = 1.0, ML = 100, and MP = 100 support are labelled with an asterisk (*), and branches with BI = 1.0, ML ≥ 95, and MP ≥ 95 are indicated with thicker branches. Posterior probability values ≥ 0.995 and < 1.0 are represented as '0.99', bootstrap support values ≥ 99.5 and < 100 are represented as '99', and bootstrap support values < 50 are indicated with two hyphens ('- -'). — Scale bar = 0.1 estimated substitutions per site.

Asian *Scolytoplatypus* symbionts formed a distinct sister group to *Ambrosiella* with strong bootstrap support, but the symbiont of *R. mutabilis* grouped with *Ambrosiella* s.str. with moderate support (Fig. 3). New ITS sequences of *Xyleborini* symbionts were placed within *Ambrosiella* s.str. (Fig. 3), as expected (Mayers et al. 2015, 2017, Lin et al. 2017).

Multi-gene Bayesian analysis confirmed the sister relationships of African *Scolytoplatypus* symbionts with *Phialophoropsis* and Asian *Scolytoplatypus* symbionts with *Ambrosiella*, as well as the placement of the *R. mutabilis* symbiont with *Ambrosiella* s.str., where it was placed as the first-diverging taxon (Fig. 7). Including *Meredithiella*, there were five distinct, well-supported clades of ambrosia fungi with high posterior probability, RAxML bootstrap, and parsimony bootstrap support values. The inferred relationships among genera in the *Ceratocystidaceae* were similar to those of previous analyses, with the ambrosia beetle symbionts, *Huntiella*, and three other species grouping separately from the other half of the family (De Beer et al. 2014, 2017, Mayers et al. 2015). The placement of *Huntiella* within the ambrosia half of the family was somewhat ambiguous. The genus was positioned under a short internode with 0.98 posterior probability support, but this branch collapsed to a polytomy when certain *Huntiella* taxa were added to or removed from analysis. The ambiguous phylogenetic placements of three lone taxa (*Bretziella fagacearum*, *Ceratocystis adiposa*, and *C. norvegica*) with respect to the ambrosia beetle symbionts were somewhat better resolved than in earlier studies (De Beer et al. 2014, 2017, Mayers et al. 2015, 2018). *Ceratocystis adiposa* was placed as sister taxon to *Meredithiella* with 1.0 posterior probability support, *B. fagacearum* formed a sister taxon to the *Phialophoropsis*/African *Scolytoplatypus* symbiont clade with moderate support, and *C. norvegica* was placed as

sister taxon to the *Ambrosiella*/Asian *Scolytoplatypus* symbiont clade with moderate support. Both *C. adiposa* and *C. norvegica* are clearly placed outside of *Ceratocystis* s.str. but are not accommodated by any currently-defined genera (De Beer et al. 2014, 2017, Mayers et al. 2015, Nel et al. 2017). Both of these species (and *B. fagacearum*) have no known close relatives, and they are biologically and morphologically distinct from each other and the ambrosia beetle symbionts.

Taxonomy

In recognition of their distinct morphological characteristics, and supported by clear phylogenetic separation from known taxa, two new genera are proposed for the respective symbionts of African and Asian *Scolytoplatypus*. The symbiont of *R. mutabilis* is described as a new species of *Ambrosiella*. Two new monotypic genera are created to accommodate the problematic non-ambrosial taxa *C. adiposa* and *C. norvegica*. An additional monotypic genus is created to accommodate a close phylogenetic relative to the *Ceratocystidaceae* isolated from a ship timber beetle gallery in the course of the study.

Wolfgangiella C. Mayers & T.C. Harr., *gen. nov.* — MycoBank MB824930

Etymology. Feminine. After entomologist Wolfgang Dietrich Schedl, who characterized the mycangia of *Scolytoplatypus* and made other significant contributions to our understanding of mycangium diversity.

Type species. Wolfgangiella franznegeri.

Irregular to spherical thallic-arthric conidia on branching hyphae that disarticulate singly or in chains, associated with ambrosia beetles, including *Scolytoplatypus* in Africa and Madagascar. Ascocarps when present spherical, pigmented, non-ostiloate, containing fusiform to falcate ascospores. Phylogenetically classified in the *Ceratocystidaceae*.

Notes — *Wolfgangiella* is most closely related to *Phialophoropsis* (Fig. 7), and its arthric-thallic conidia are somewhat similar to the disarticulating cells observed in *Phialophoropsis* (Mathiesen-Käärik 1953). However, all studied *Phialophoropsis* spp. produce chained conidia from deep-seated phialides (Batra 1967, Mayers et al. 2015), which were not observed in *Wolfgangiella*. Cultures of the type species for *Wolfgangiella* produce significantly less pigment than *Phialophoropsis* spp.

Wolfgangiella franznegeri C. Mayers, T.C. Harr., & Roets, *sp. nov.* — MycoBankMB 824932; Fig. 2a–m, 6l

Etymology. After the German botanist Franz Wilhelm Neger (1868–1923), an early pioneer in the study of the ambrosia beetle symbiosis.

Typus. South Africa, Western Cape Province, Betty's Bay, Harold Porter National Botanical Garden, S34°21'1.58" E18°55'37.03", from mycangium of *Scolytoplatypus fasciatus* caught in flight, 21 Jan. 2017, *F. Roets* (BPI 910639 holotype, dried culture), culture ex-type CBS 144149 (= C4328).

Ascomata embedded in mounded mycelium, cleistothecious, spherical, brown, *textura intricata*, 28–142 µm diam at maturity, lacking necks or ostioles. *Asci* not observed. *Ascospores* 33–60 × 7–19 µm, thick-walled, fusiform to falcate. *Conidiophores* 14–66 µm long, composed of branching, disarticulating chains of thallic-arthric conidia. *Conidia* irregular to globose, 6–16(–32) × 4.5–13(–32) µm, detaching singly or in linear or branching chains.

Cultural characteristics — Colonies on MYEA 5–25 mm after 7 d at 25 °C, odour sweet, margin submerged, hyaline to olivaceous buff with olivaceous clumps, reverse buff to isabelline to pale mouse grey, surface growth aerial, white to pale olivaceous grey, with superficial white spherical sporodochia in clusters bearing tufts of conidiophores.

Additional specimens examined. Madagascar, Andasibe-Mantadia National Park, ambrosia growth in gallery of *Scolytoplatypus rugosus* in *Ocotea* sp., May 2015, *B. Jordal* BPI 910640. – South Africa, Western Cape, Diepwalle Forest Station, propagules in mycangium of *S. fasciatus* in unidentified tree, Nov. 2007, *B. Jordal* sp2.

Additional cultures examined. South Africa, Western Cape Province, Betty's Bay, Harold Porter National Botanical Garden, from mycangium of *Scolytoplatypus fasciatus* caught in flight, 21 Jan. 2017, *F. Roets* C4325; Western Cape Province, Betty's Bay, Harold Porter National Botanical Garden, from mycangium of *S. fasciatus* caught in flight, 21 Jan. 2017, *F. Roets* five isolates from separate females (C4325, C4326, C4327, C4329, C4331).

Notes — Six of six females of *S. fasciatus* trapped in flight in South Africa yielded *W. franznegeri*, and it dominated a gallery of *S. rugosus* in Madagascar. *Scolytoplatypus fasciatus* and *S. rugosus* are close relatives, but the former is only known from South Africa and the latter from a small area in Madagascar (Jordal 2013). ITS sequences from all sources were identical (Fig. 1).

Wolfgangiella madagascarensis C. Mayers, McNew, & T.C. Harr., *sp. nov.* — MycoBank MB824933; Fig. 2n–t

Etymology. After the country of origin, Madagascar.

Typus. Madagascar, Ambohitantely Forest Reserve, ambrosia growth in gallery of *Scolytoplatypus permirus* in *Ocotea* sp. or *Macaranga* sp., May 2015, *B. Jordal* (BPI 910641 holotype).

Conidiophores composed of branching, disarticulating chains of thallic-arthric conidia. *Conidia* irregular or globose to subglobose, 4–13.5(–17) µm diam, detaching singly or in chains. *Growth in mycangium* composed of irregular cells 4.5–12.5 × 3.5–7 µm in size, solitary or in branched or unbranched chains.

Additional specimens examined. Madagascar, Ranomafana National Park, propagules in mycangium of *Scolytoplatypus permirus* caught in flight, 2012, *B. Jordal* sp3; Andasibe-Mantadia National Park, ambrosia growth in gallery of *S. permirus* in *Ocotea* or *Macaranga* sp., May 2015, *B. Jordal* M399.

Notes — *Wolfgangiella madagascarensis* was observed in galleries from two locations in Madagascar and detected by ITS sequence analysis at another location, all associated with *S. permirus*, which is only known from Madagascar (Jordal 2013). The ITS sequence obtained from the mycangium contents differed by a two-base repeat in the first variable region compared to the sequences from galleries (Fig. 1). The DNA sequences of *W. madagascarensis* and *W. franznegeri* differed slightly in the ITS region (Fig. 1) and in the multi-gene alignment (one insertion in 18S rDNA, three substitutions in *tef*1-α, one insertion in the *tub* intron, and one substitution in *mcm7*). Aside from the presence of ascomata and ascospores in *W. franznegeri* cultures, the two species of *Wolfgangiella* are morphologically similar.

Toshionella C. Mayers & T.C. Harr., *gen. nov.* — MycoBank MB824934

Etymology. Feminine. After Toshio Nakashima, who contributed the majority of our previous knowledge on Asian *Scolytoplatypus* symbionts.

Type species. Toshionella nipponensis.

Aleurioconidia terminal, thick-walled, globose, single or in basipetal chains, sometimes surrounded by a membranous sheath, on branching monilioid or simple conidiophores. Associated with ambrosia beetles, including *Scolytoplatypus* spp. in Asia. Phylogenetically classified in the *Ceratocystidaceae*.

Notes — One or more members of this genus were previously reported from Asian *Scolytoplatypus* and treated as putative species of *Ambrosiella* (Nakashima et al. 1987, 1992, Nakashima 1989, Kinuura et al. 1991, Kinuura 1995, Beaver & Gebhardt 2006). *Toshionella* is closely related to *Ambrosiella*

(Fig. 7), and its conidiophores are similar, but its aleurioconidia are much larger. The phialidic conidiophores reported in *Ambrosiella* (Lin et al. 2017, Mayers et al. 2015, 2017) were not observed in *Toshionella*. The thin membranous sheath observed around chains of aleurioconidia (Fig. 4h, s–t) has been reported in *A. cleistominuta* (Mayers et al. 2017) and *C. adiposa* (Hutchinson 1939, Bhat 1972, Hawes & Beckett 1977a, b). Though rare, *Toshionella* aleurioconidia sometimes disarticulate with the penultimate conidiophore cell attached (Fig. 4e, j, v), as is common in *Ambrosiella* and *Meredithiella* (Harrington et al. 2014, Mayers et al. 2015, 2018). All *Toshionella* cultures produced wet and gooey mounds of thick-walled, globose to irregular, hyaline cells (Fig. 4f, n, w), which may be the 'sprout cells' previously reported forming a 'slimy layer' in galleries of *Scolytoplatypus* spp. (Nakashima 1989, Beaver & Gebhardt 2006).

Toshionella nipponensis C. Mayers, T.C. Harr., & H. Masuya, *sp. nov.* — MycoBank MB824935; Fig. 4a–f

Etymology. After the country of origin, Japan (endonym Nippon).

Typus. Japan, Akita prefecture, Tazawako, from mycangium of *Scolytoplatypus shogun* emerging from *Fagus crenata*, July 2014, *H. Masuya* (BPI 910635 holotype, dried culture), culture ex-type CBS 141492 (= C3904).

Conidiophores 8.5–35 µm long, single- or multiple-celled, hyaline becoming red-brown, branched, composed of thick-walled monilioid cells, bearing terminal aleurioconidia, conidiophore cells later becoming thick-walled and disarticulating into single cells. *Aleurioconidia* hyaline becoming faintly red-brown, globose to subglobose, ovoid, 18–26 × 17.5–25.5 µm, generally wider than tall, often flat on bottom, borne singly or in chains, terminally, from monilioid conidiophores, terminally or intercalary on simple hyphae, or rarely directly from the side of conidiophore. In older cultures, thick-walled cells presumed to be aleurioconidia accumulate in moist mounds on the culture surface, globose to ellipsoidal, thick-walled, 7–25 µm diam.

Cultural characteristics — Colonies on MYEA 32–55 mm after 7 d at 25 °C, surface growth white, fluffy in patches, later covering surface and becoming chalky, pale olivaceous to olivaceous grey, reverse grey olivaceous to olivaceous black, becoming dark slate blue, margin hyaline, becoming greenish black. In older cultures, irregular buff sporodochia on surface, sometimes bearing red liquid drops, later center growth thick, dense, raised, and red-brown.

Additional cultures examined. Japan, Akita prefecture, Tazawako, from mycangium of *Scolytoplatypus shogun* emerging from *Fagus crenata*, July 2014, *H. Masuya* three isolates from separate females (C3905, C3906, C3907); Iwate prefecture, Hachimantai, from mycangium of *S. shogun* emerging from *Fagus crenata*, 7 July 2014, *H. Masuya* C4064.

Notes — *Toshionella nipponensis* was isolated from five *S. shogun* females in Japan, and the cultures had an identical ITS sequence that was nearly identical to those obtained from Japanese *S. daimio*, *S. mikado*, and *S. shogun* isolates in 2002 (Fig. 3). The fungus illustrated in galleries of Japanese *S. daimio*, *S. mikado*, and *S. shogun* (Nakashima et al. 1987, 1992, Nakashima 1989, Kinuura et al. 1991, Kinuura 1995) and informally described by Nakashima et al. (1987) is probably *T. nipponensis.* Sequences obtained from Japanese *S. mikado* by Ito & Kajimura (2017), including sequences of 18S rDNA (LC140888), 28S rDNA (LC140895 and LC140896), and *tub* (LC140904), may also represent *T. nipponensis*. An atypical isolate from *S. shogun* that differed in phenotype, DNA sequences, and culture morphology is described below as a separate species.

Toshionella transmara C. Mayers, T.C. Harr. & H. Masuya, *sp. nov.* — MycoBank MB824936**;** Fig. 4g–p

Etymology: After Latin transmara (adj) 'sea-crossing', as it was detected from both sides of the Sea of Japan.

Typus. Japan, Iwate prefecture, Hachimantai, from mycangium of *Scolytoplatypus shogun* emerging from *Fagus crenata*, June 2015, *H. Masuya* (BPI 910638 holotype, dried culture), culture ex-type CBS 141493 (= C3908).

Conidiophores 8–40 µm long, single- or multi-cellular, hyaline, branched, composed of thick-walled monilioid cells, bearing terminal aleurioconidia, conidiophore cells later becoming thick-walled, disarticulating into single cells. *Aleurioconidia* hyaline, thick-walled, globose to subglobose, ovoid, (8.5–)14–18 × (8.5–)14–19 µm, generally wider than tall, often flat on bottom, borne singly or in chains, terminal on monilioid conidiophores or on single-celled side branches, or rarely directly from the side of conidiophores. Thick-walled cells presumed to be aleurioconidia occasionally accumulate in moist mounds on the culture surface, globose to ellipsoidal, thick-walled, 10.5–30 µm diam. *Thallic-arthric conidia* thick-walled, 11–17(–19.5) × 9–13.5(–16) µm, usually ellipsoidal to globular, borne in branching monilioid chains on the surface of mature sporodochia, disarticulating singly or in chains. *Mycangial growth* of branching, thallic-arthric cells, 4.5–10 × 5–14 µm, solitary or in chains.

Cultural characteristics — Colonies on MYEA 40–63 mm after 7 d at 25 °C, surface growth superficial, greyish sepia to olivaceous grey, covered in randomly dispersed superficial, spherical, white to off-white sporodochia 1–1.2 mm diam, distributed randomly, in concentric rings, or clustered around site of transfer, reverse greenish black, margin greenish black, aerial hyphae absent.

Additional specimens examined. Russia, Vladivostok, propagules in mycangium of *Scolytoplatypus tycon* caught in flight, July 2008, *B. Jordal* sp1.

Notes — This species is closely related to *T. nipponensis* (Fig. 3) but can be differentiated by its faster rate of growth, scattered spherical sporodochia, and lack of chalky white surface growth. The single living representative (C3908 = CBS 141493) was isolated from *S. shogun* in Japan, but nearly-identical ITS sequences were obtained from the mycangium of a female *S. tycon* caught in Vladivostok, Russia (sp1) and three cultures from Japanese *S. tycon* sequenced in 2002 (Fig. 3). Nakashima et al. (1992) may have illustrated *T. transmara* in galleries of Japanese *S. tycon*.

Toshionella taiwanensis C. Mayers, T.C. Harr. & H.H. Shih., *sp. nov.* — MycoBank MB824937; Fig. 4q–z

Etymology. After the location of first discovery, Taiwan.

Typus. Taiwan, Kaohsiung City, Douna, from *Scolytoplatypus pubescens* caught in flight, Feb. 2014, *H.H. Shih* (BPI 910637 holotype, dried culture), culture ex-type CBS 141494 (= C3687).

Conidiophores 15–115 µm long, hyaline or red-brown, branched, composed of thick-walled monilioid cells or thin-walled irregular cells, produced densely across the entire surface of the culture, bearing terminal aleurioconidia, conidiophore cells developing into thick-walled chlamydospores. *Aleurioconidia* hyaline, thick-walled, globose to subglobose, ovoid, 13.5–23 × 12.5–22 µm, generally wider than tall, often flat on bottom, produced terminally, singly or in chains, on long monilioid conidiophores or single-celled side branches or directly on simple hyphae. *Chlamydospores* of two types, borne terminally on branching, aerial, erect towers of simple hyphae, thick-walled, globose to subprolate, obovoid, deeply pigmented, 15.5–18 × 15–16 µm, generally taller than wide; or ellipsoidal to globular, lightly red-brown, thick-walled, disarticulating singly or in chains, borne in

branching monilioid chains. In older cultures, thick-walled cells presumed to be aleurioconidia accumulate in moist mounds on the culture surface, globose to ellipsoidal, thick-walled, 10.5–26.5 µm diam. *Mycangial growth* branching, thallic-arthric, of thick-walled cells, 4.5–11.5 × 3.5–8 µm, solitary or in chains.

Cultural characteristics — Colonies on MYEA (22–)40–53 mm after 7 d at 25 °C, reverse greenish black, margins hyaline to buff, submerged, becoming white, dense, raised, fruity smell at 5 d, somewhat fading by 14 d, covered with a dense white to olivaceous grey carpet of aerial mycelium and conidiophores. Subsurface hyphae visible beneath the dendroid margin of surface growth, deeply pigmented with diffusible pigment rarely extending beyond surface growth, deep brown to greenish black.

Additional cultures examined. Taiwan, Kaohsiung City, Jingdashan, from *Scolytoplatypus pubescens* caught in flight, Feb. 2014, *H.H. Shih* C3688; Nantou County, Lienhuachih, from *S. mikado* caught in flight, Aug. 2014, *C. Wuest* CBS 141495 (= C3448; dried culture BPI 910636).

Additional specimens examined. Taiwan, Nantou County, Lienhuachih, propagules in mycangium of *Scolytoplatypus mikado* caught in flight, June 2014, *H.H. Shih* M304; Yilan County, Fushan, propagules in mycangium of *S. mikado* in *Cinnamomum* sp., June 2014, *H.H. Shih* M305.

Notes — This new species is associated with both *S. pubescens* and *S. mikado* in Taiwan and is related to the Japanese *Toshionella* species (Fig. 3). Sequences obtained in 2002 from Japanese *S. mikado* were of *T. nipponensis* rather than *T. taiwanensis*, implying geographic rather than host-species distinction of the two species (Fig. 3). *Toshionella taiwanensis* can be differentiated from the Japanese *Toshionella* by its dense, fluffy surface growth and the presence of upright, branching aerial towers bearing terminal, pigmented chlamydospores (Fig. 4x–y), which are unique among the studied ambrosia fungi but similar to the aleurioconidia produced by species of *Ceratocystis* s.lat. (Paulin-Mahady et al. 2002). The fungus isolated from *S. pubescens* in Taiwan by Lin (2016) and given the provisional name '*Ambrosiopsis globosa'* is probably *T. taiwanensis.* The isolate from *S. mikado* (C3448 = CBS 141495) initially resembled the two isolates from *S. pubescens*, but C3448 later grew more slowly (32–36 mm after 7 d at 25 °C with a maximum growth diameter of 63–67 mm) and produced a diffusible red-brown pigment that was not observed in the other isolates. The changed culture also lacked fluffy surface growth, instead forming conidiophores in loose tufts across the surface and below the surface of the agar. Cultures obtained from *S. raja* caught in mainland China had ITS sequences identical to those of *T. taiwanensis* (Fig. 3), suggesting that the species is not restricted to Taiwan, but further study of the cultures is needed. A very similar sequence was obtained from a *S. eutomoides* female in Papua New Guinea (Fig. 3).

Ambrosiella Brader ex Arx & Hennebert emend. C. Mayers & T.C. Harr.

Etymology. Brader (1964) named the genus for its ecological role as 'ambrosia', a term first coined by Schmidberger (1836).

Type species. *Ambrosiella xylebori*.

Conidiophores single to aggregated in sporodochia, hyaline, unbranched or sparingly branched, one-celled to septate, producing terminal aleurioconidia or chains of conidia from phialides. *Ascomata*, when present, cleistothecious, *textura intricata*. *Ascospores* hyaline, aseptate, reniform, often thick-walled. *Asci* not observed. Associated with ambrosia beetles. Phylogenetically classified in the *Ceratocystidaceae*.

Notes — Harrington et al. (2010) restricted *Ambrosiella* to ambrosia beetle symbionts related to *Ceratocystis* (i.e., classified in *Ceratocystidaceae*). Mayers et al. (2015) showed *Ambrosiella* to be polyphyletic and returned *A. ferruginea* and *A. trypodendri* to *Phialophoropsis*. Mayers et al. (2017) demonstrated a cleistothecious sexual morph in *A. cleistominuta*, as we demonstrated here in the type species, *A. xylebori.* The generic description of *Ambrosiella* is here emended and follows the asexual description of Harrington et al. (2010), and is updated to include the morphology of its sexual morph. The ten current species include the seven *Xyleborini*-associated species reviewed by Mayers et al. (2015), as well as two other *Xyleborini*-associated species (Lin et al. 2017, Mayers et al. 2017) and the new species described below.

Ambrosiella remansi C. Mayers & T.C. Harr., *sp. nov.* — MycoBank MB824938; Fig. 5c–d

Etymology. After *Remansus*, the genus from which the only known specimen was associated.

Typus. Madagascar, Andasibe-Mantadia National Park, propagules in mycangium of female *Remansus mutabilis*, May 2015, *B. Jordal* (BPI 910622 holotype).

Growth in mycangium composed of thallic-arthric cells 6–13 × 4–10 µm in size, globose to irregular in shape, single or in chains of two or more cells.

Notes — This species was found as propagules in the mycangium of *R. mutabilis*, the type species for the genus *Remansus*, which is only known from Madagascar (Jordal 2013). The ITS sequence obtained from this single specimen places it with *Ambrosiella* (Fig. 3), and the multigene phylogeny places the fungus as an early-diverging member of *Ambrosiella* (Fig. 7). Though its conidial morph is unknown, the mycangial growth of *R. remansi* is composed of non-branched, thallic-arthric mycangial propagules as expected of *Ambrosiella* (Harrington et al. 2014, Mayers et al. 2015, 2017), in contrast to the more irregular and sometimes-branching mycangial growth of *Toshionella.* The rarity of *Remansus* specimens (Jordal 2013) precludes further study at this time, but the novelty of the first *Ambrosiella* sp. not associated with the mesonotal mycangium of a host in the *Xylosandrus* complex warrants the naming of *A. remansi* as a new species.

Catunica C. Mayers & T.C. Harr., *gen. nov.* — MycoBank MB824939

Etymology. Feminine. An arbitrary construction based on the Latin catena (n), chain; and tunica (n), tunic/membrane.

Type species. Catunica adiposa.

Perithecia black, with long necks, ostiolar hyphae hyaline to brown. *Ascospores* hyaline, half-moon-shaped, sometimes with a sheath. *Conidiophores* phialidic, hyaline to brown, producing chains of conidia that vary from hyaline to pale brown, cylindrical to doliiform, or with truncate to rounded ends, smooth-walled to verrucose. *Aleurioconidiophores* enteroblastic to holoblastic, pigmented, producing chains of dark brown to black *aleurioconidia*, ovoid to globose, thick-walled, with verrucose to fimbriate walls, often enveloped by a brown membranous sheath, detaching in chains, with or without sheath. Phylogenetically classified in the *Ceratocystidaceae*.

Notes — *Catunica adiposa*, the only known species of the genus, is a causal agent of sugar cane rot (Butler 1906, Sartoris 1927), has been implicated in human illness (Agarwal et al. 2014), and has been isolated from *Prunus* (Paulin-Mahady et al. 2002), *Pinus* (Talbot 1956), air (e.g., CBS 138.34), books (e.g., IMI 21285), and other substrates. *Catunica* has distinctive variation in conidium morphology, ranging from typical cylindrical conidia from deep-seated phialides (endoconidia) to thick-walled, dark, ornamented aleurioconidia (Fig. S1).

These conidial types were referred to as phialoconidia and chlamydospores by Nag Raj & Kendrick (1975). We agree with other authors (Butler 1906, Sartoris 1927, Davidson 1935, Moreau 1952, Hunt 1956, Talbot 1956, Upadhyay 1981) that both types of spores are produced from common conidiophores and change over time. It may produce the longest perithecium necks in the family (Malloch & Blackwell 1993) and also produces distinctive, half-moon-shaped ascospores with gelatinous sheaths. Its ecology and phylogenetic position are unique (Fig. 7), and its relationship to *Meredithiella* spp., which are obligate symbionts of ambrosia beetles (Mayers et al. 2018), is difficult to reconcile.

Catunica adiposa (E.J. Butler) C. Mayers & T.C. Harr., *comb. nov.* — MycoBank MB824940; Fig. 6a, S1a–S1e

Basionym. Sphaeronaema adiposum E.J. Butler, Mem. Dept. Agric. India, Bot. Ser. 1: 40. 1906.

Synonyms. Ceratostomella adiposa (E.J. Butler) Sartoris, J. Agric. Res. 35: 585. 1927.

Ophiostoma adiposum (E.J. Butler) Nannf. in Melin & Nannf., Svenska Skogsv.-Fören. Tidskr. 32: 408. 1934.

Endoconidiophora adiposa (E.J. Butler) R.W. Davidson, J. Agric. Res. 50: 802. 1935.

Ceratocystis adiposa (E.J. Butler) C. Moreau, Rev. Mycol. (Paris) Suppl. Col. 17: 22. 1952.

Ceratostomella major J.F.H. Beyma, Zentrabl. Bakteriol., 2. Abt. 91: 348. 1935.

Ophiostoma majus (J.F.H. Beyma) Goid., Boll. Staz. Patol. Veg. Roma 15: 158. 1935.

Ceratocystis major (J.F.H. Beyma) C. Moreau, Rev. Mycol. (Paris) Suppl. Col. 17: 22. 1952.

Etymology. After the 'fatty substance' in which the ascospores are suspended (Butler 1906).

Typus. Canada, Ontario, Cornwall, from hardwood chips, 14 Jan. 1969, *J.K. Shields* (BPI 910979, epitype designated here MBT386138, dried culture), culture ex-epitype CBS 183.86 (= C999 in collection of T.C. Harrington = C251B/C411 in collection of FPInnovations/Forintek). – India, Bihar, Champaran, Seeraha, on *Saccharum officinarum*, 30 Oct. 1903, *E.J. Butler* HCIO 3531 lectotype designated here, MBT386139.

For descriptions, see Butler (1906), Sartoris (1927), Davidson (1935), Moreau (1952), Hunt (1956), Talbot (1956), Nag Raj & Kendrick (1975), and Upadhyay (1981).

Additional cultures examined. France, 1953, *C. Moreau* CBS 147.53 (= C905 = LCP 903). – India, from *Saccharum officianarum*, date unknown (deposited in IMI prior to 1927; deposited in CBS in 1927; deposited in MUCL in 1967), *Subramanian* CBS 127.27 (= C997 = MUCL 9507). – Japan, from *Prunus persica*, date unknown, *P. Soentoro* CBS 600.74 (C998). – Netherlands, from air, c. 1934, *F.H. van Beyma* CBS 138.34 (= C906 = MUCL 9518). – USA, North Carolina, from wood chips, 1987, *R.A. Blanchette* C299.

Notes — Butler (1906) did not designate a type specimen, but he established Herbarium Cryptogamae Indiae Orientalis (HCIO) in 1905 (Maheswari et al. 2012) and deposited a specimen (HCIO 3531) under the name *Sphaeronaema adiposum*. The specimen is available in HCIO, which is maintained by the Division of Plant Pathology, ICAR-Indian Agricultural Research Institute, New Delhi, India (pers. comm., HCIO). The collection information for HCIO 3531, 1903 in Bihar (Fig. S2a), matches his first discovery of the fungus (Butler 1906) and the specimen consists of an infected section of sugarcane with red-brown streaks and dark black fungal growth (Fig. S2b), consistent with Butler's description of *S. adiposum*. This is the only specimen known to be directly identified by Butler as *S. adiposum*, it appears to be part of the protologue, and we designate HCIO 3531 as lectotype for the species (see Fig. S3 and caption for discussion of IMI 21355 and IMI 21285, the only reasonable alternatives). We did not examine HCIO 3531, but six isolates of *C. adiposa* from six different countries (Table S1) had identical ITS sequences (Fig. 3) and displayed the characteristic conidiophores and conidia of *C. adiposa* (Fig. S1), as illustrated by Butler (1906), Hunt (1956) and Nag Raj & Kendrick (1975). We designate a dried culture of CBS 183.86 from Canada as epitype, and it was used to represent *C. adiposa* in our multi-locus phylogenetic analyses and produced sexual and asexual structures in culture. Isolate CBS 127.27 (= MUCL 9507) was collected in India on *Saccharum officinarum*, and it shares the common ITS sequence of the other isolates, but our culture of CBS 127.27 was sterile and debilitated. A draft genome (ASM164068v1) is available for *C. adiposa* CBS 136.34 (Wingfield et al. 2016a), and an NCBI BLASTn search against this genome using our ITS sequence found a perfect match (460/460 bp identical).

Solaloca T.C. Harr., *gen. nov.* — MycoBank MB824941

Etymology. Feminine. An arbitrary construction based on the Latin sola (adj), feminine form of solus, 'solitary'; and locus (n), 'place/location'.

Type species. Solaloca norvegica.

Perithecial bases and necks black, ostiolar hyphae hyaline. *Ascospores* hyaline, thick-walled, cylindrical to rarely curved. *Conidiophores* not observed. Phylogenetically classified in the *Ceratocystidaceae*.

Notes — *Solaloca norvegica* was isolated from a single collection of galleries of *Ips typographus* in *Picea abies* in Norway in 1974, but the new species was not described until 2010 (Reid et al. 2010). Conidia were not seen, and we failed to find conidia in our isolate (C4124) of the ex-type strain UAMH 9778 (= UAMH 11187). Phylogenetically, *Solaloca* is placed within the family *Ceratocystidaceae* (Fig. 7) with no obvious relatives. In morphology (perithecia and ascospores) and habitat, it resembles the conifer-inhabiting members of *Endoconidiophora* (Harrington & Wingfield 1998), and it shares no obvious characters with ambrosia beetle symbionts other than the association with the subfamily *Scolytinae*.

Solaloca norvegica (J. Reid & Georg Hausner) T.C. Harr., *comb. nov.* — MycoBank MB824942; Fig. 6f

Basionym. Ceratocystis norvegica J. Reid & Georg Hausner, Botany 88: 977 (2010).

Etymology. After the country of origin, Norway (Reid et al. 2010).

Typus. Norway, Ostfold, near Sandem, from gallery of *Ips typographus* in *Picea abies*, Sept. 1973, *J. Reid* (UAMH 11187 holotype, dried culture), ex-type culture under same accession.

For description, see Reid et al. (2010).

Additional cultures examined. Norway, Ostfold, near Sandem, from gallery of *Ips typographus* in *Picea abies*, Sept. 1973, *J. Reid* UAMH 9778.

Note — We examined strain UAMH 9778 (a duplicate of the holotype/ex-type UAMH 11187) and found its characters to be consistent with the original description.

Inodoromyces C. Mayers & T.C. Harr., *gen. nov.* — MycoBank MB828237

Etymology. Masculine. After the Latin inodorus (adjective, 'without scent') and -myces ('fungus').

Type species. Inodoromyces interjectus.

Conidia terminal, chained or clustered, from phialidic conidiophores on simple hyphae. Phylogenetically classified in the *Microascales*. Sexual morph unknown.

Notes — *Inodoromyces* lacks the odour and pigmentation characteristic of much of the *Ceratocystidaceae*, to which it forms

an *incertae sedis* sister group (Fig. 7), but it shares phialidic conidiogeny with the *Ceratocystidaceae*. The genus is based on only one isolate, but its unique phylogenetic position between the *Ceratocystidaceae* and the *Gondwanamycetaceae* (e.g., *Knoxdaviesia*) merits its description. Although our phylogenetic analyses did not include the mycophilic *Microascales* genus *Cornuvesica*, which is also family *incertae sedis* and related (on a long branch) to both the *Ceratocystidaceae* and *Gondwanamycetaceae* (Marincowitz et al. 2015), *Cornuvesica* spp. cannot grow independently and the 18S sequence of *I. interjectus* C3547 differed significantly from that of *Cornuvesica falcata* (1545/1661 bases, 93 % match with AY271797) (Hausner & Reid 2004).

Inodoromyces interjectus C. Mayers & T.C. Harr., *sp. nov.* — MycoBank MB828238; Fig. 8

Etymology. Based on the Latin interjectio (noun, alternative form of interiectio, 'interjection'), after the terminal pairs of conidia in early conidiophores (Fig. 8c–d) that often resemble an exclamation mark (!).

Typus. USA, Michigan, Montcalm County, Alma College Ecological Tract, from gallery of *Elateroides lugubris* larvae in *Populus* sp., Dec. 2014, *M. Bunce* (BPI 910978 holotype, dried culture), culture ex-type CBS 142647 (= C3547).

Conidiophores hyaline, simple to many-branched, scattered across surface and embedded in media, bearing terminal conidia from deep phialides in chains, forming clusters. *Conidia* hyaline, 3–12(–30) × 1.5–4.5 µm, globose becoming oblong (rarely bacilliform) with increasing size, often with one or two conspicuous polar vacuoles, rarely septate. *Gallery growth* sparse tufts of condiophores, similar to those in culture.

Cultural characteristics — Colonies on MYEA 30–48 mm diam after 4 d at 25 °C, surface growth superficial, hyaline, margin dendroid, irregularly branched, submerged, extending further than surface, lacking odour, reverse hyaline.

Notes — We interpret *I. interjectus* as a transient contaminant rather than a symbiont of the ship timber beetle *E. lugubris*. We also isolated an *Alloascoidea* sp. (CBS 142651) with a 28S sequence (MK025991) similar to *A. hylecoeti* (563/589 bp, 96 %, match with NG_055394; Kurtzman & Robnett 2013) that dominated growth in the gallery and is the presumptive mycangial symbiont of *E. lugubris* (Batra & Francke-Grosmann 1961, 1964, Kurtzman & Robnett 2013).

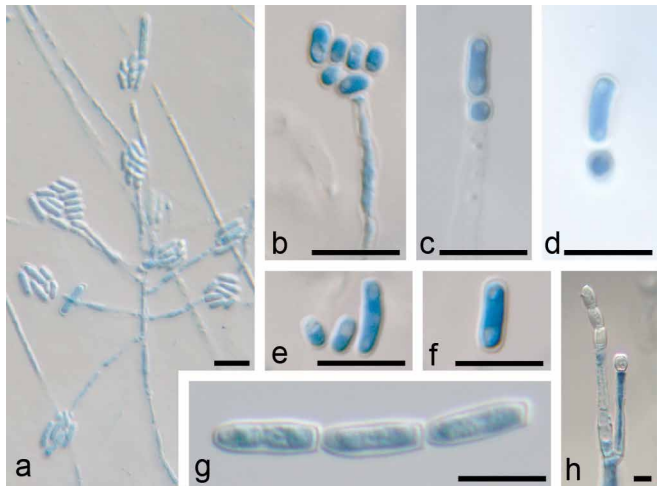

Fig. 8 *Inodoromyces interjectus*. a. Branched conidiophore; b. cluster of conidia grouped at mouth of phialide; c. long/short conidium pair at terminal end of young conidiophores; d–g. conidia; h. conidiophore with conidia (all photos (except h) by Nomarski interference microscopy of CBS 142647 embedded in malt yeast extract agar, stained with cotton blue; h from gallery walls of *Elateroides lugubris*). — Scale bars = 10 µm.

DIVERGENCE DATE COMPARISONS

The topology of the *Ceratocystidaceae* in the time-calibrated tree produced by BEAST (Analysis A, Fig. S4) was identical to that of the MrBayes tree (Fig. 7). Median age estimates and 95 % HPD ranges were produced for all nodes in the tree using secondary fossil dates (Fig. S4, Table 2). Most of the estimates produced by Analysis B (fixed molecular clock based on 18S sequences at 1.25 % substituions per 100 Ma) fell within the 95 % HPD ranges of Analysis A, with the exception of crown ages of genera, where 18S rDNA variation was very limited. Analysis B gave an older estimate for the crown of the family *Ceratocystidaceae* (Table 2), but otherwise Analysis B estimates were younger or approximated those in Analysis A, and the chronological order of the node dates were similar in the two analyses. The estimated crown age for the *Ceratocystidaceae* at 80.3 Ma using Analysis A was somewhat older than the estimate of 61.9 Ma by Van der Nest et al. (2015), who used a similar secondary analysis and calibration points but many fewer taxa.

The clade accommodating all ambrosia fungi in the family (node 1, Fig. 9) had an estimated crown age of 62.4 Ma, older than the

Table 2 Comparison of divergence date estimates generated for selected fungal clades and available divergence date estimates for the beetle clades with large mycangia.

Clade	Beetle divergences[1]	Fungal Analysis A[2]	Fungal Analysis B[3]
Ceratocystidaceae		80.3 (53.7, 115.5)	103.9
Ambrosia common ancestor (node 1)		62.4 (41.1, 91.3)	51.8
Scolytoplatypodini (pronotal disk mycangium)	53.8 (48.7, 61.2)		
Meredithiella/*Toshionella*/*Ambrosiella* (node 2)		46.7 (30.0, 69.6)	46.4
Scolytoplatypus (split of African/Asian setal types)	41.1 (36.3, 50.7)		
Wolfgangiella/*Phialophoropsis* (node 3)		31.2 (16.2, 52.4)	19.6
Toshionella/*Ambrosiella* (node 4)		30.5 (18.1, 47.4)	34.1
Ambrosiella including *A. remansi* (node 5)		18.1 (8.7, 29.6)	4.8
Tribe Xyleborini	< 14.3 (13, 15.5)[4]		
Ambrosiella excluding *A. remansi*		12 (5.1, 21.2)	2.4
Corthylus (prothoracic coil mycangium)	16.4 (5.6, 29.7)		
Meredithiella		16.6 (7.3, 30.7)	19.4
Trypodendron (prothoracic pleural mycangium)	11.6 (9.6, 13.3)		
Phialophoropsis		5 (1.9, 10.3)	< 0.04

[1] Estimates from 29-partition analysis of Pistone et al. 2018, except *Corthylus* from Gohli et al. 2017; median crown age (low 95 % HPD, high 95 % HPD).
[2] Analysis A: Six-locus BEAST analysis; median crown age (low 95 % HPD, high 95 % HPD).
[3] Analysis B: 18S fixed rate analysis; crown age at 1.25 %/100 Ma.
[4] Estimate is for entire tribe *Xyleborini*; the *Xylosandrus* complex (mesonotal mycangium origin) would be slightly younger.

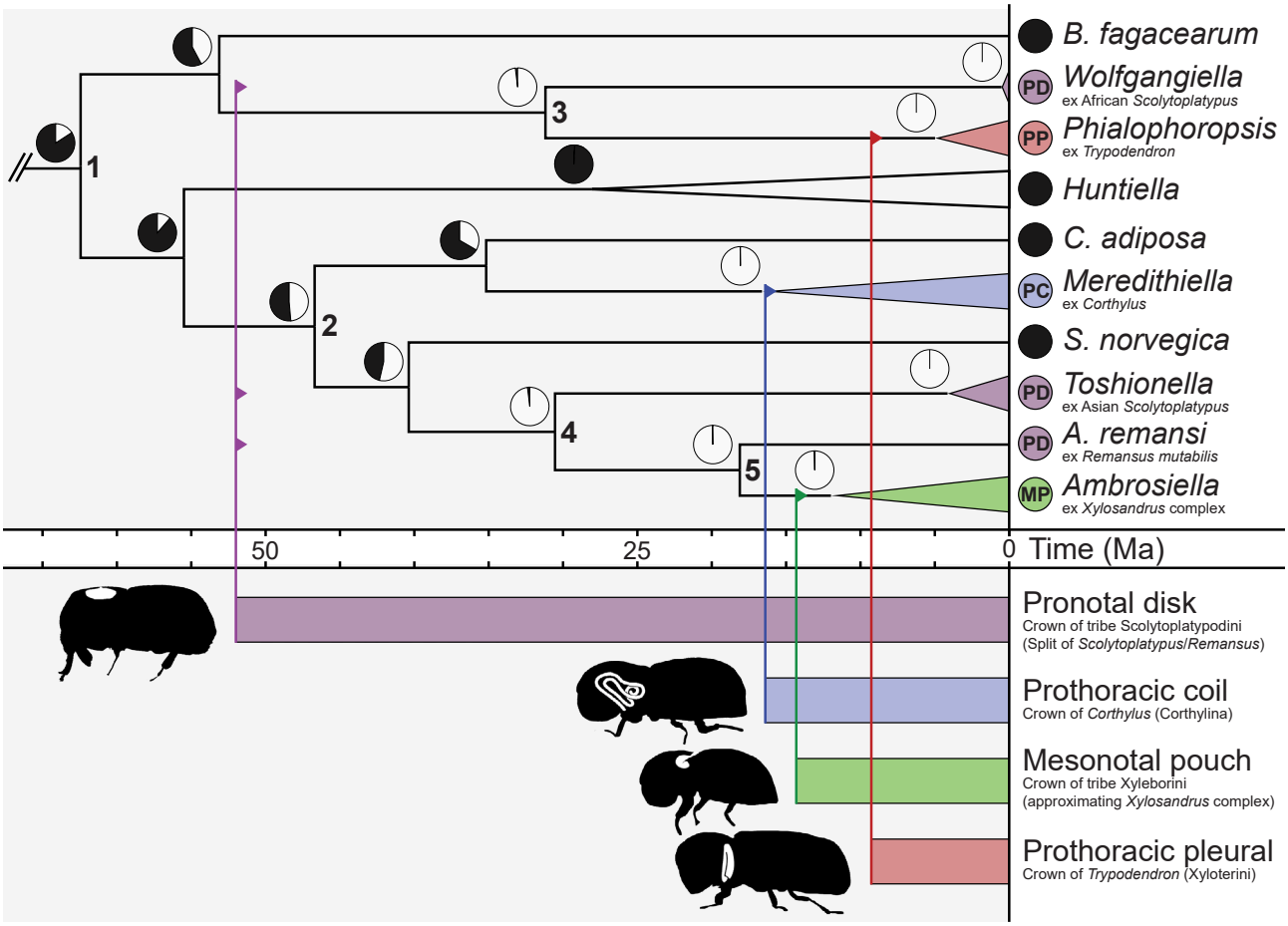

Fig. 9 Ancestral state reconstruction and estimated divergence dates of ambrosia fungi in the *Ceratocystidaceae* (top) compared to the estimated origins of the mycangia of their associated ambrosia beetle hosts (bottom). The tree is excerpted from the dated phylogenetic tree in Fig. S4, with genera of ambrosia beetle symbionts (coloured circles with abbreviations for associated mycangium type) and related non-ambrosial genera (black circles). Ambrosial clades represented by more than one species are represented by triangles, with the left apex of the triangle at the crown age of the genus. Pie charts above each node indicate the relative probabilities from ancestral state reconstruction for an ambrosial (white) or non-ambrosial (black) lifestyle. Nodes discussed in the text are labeled 1–5. Bar graph below represents the estimated divergence dates for each of the indicated mycangium types (Gohli et al. 2017, Pistone et al. 2018), which are illustrated by beetle silhouettes to the left of each bar. Right-facing flags on the vertical lines extending from the bars indicate fungal taxa associated with that mycangium type. Horizontal scale is in millions of years ago (Ma).

estimate for the origin of the oldest large mycangium (i.e., the pronotal disk mycangium of the *Scolytoplatypodini*) at 52 Ma (Pistone et al. 2018), though the 95 % HPD ranges overlapped (Table 2). The estimated crown age for the clade containing all ambrosia fungi with aleurioconidia, that is, *Ambrosiella*, *Meredithiella*, and *Toshionella* (node 2, Fig. 9), was 46.7 Ma, which is somewhat younger than the Pistone et al. (2018) estimated age for the pronotal disk mycangium (*Scolytoplatypodini*) but is much older than the estimated ages for the mesonotal (*Xylosandrus* complex) and prothoracic coil (*Corthylus*) mycangia. The estimated crown age for the *Wolfgangiella* and *Phialophoropsis* split (node 3, Fig. 9) at 31.2 Ma is somewhat younger than the estimated African-Asian *Scolytoplatypus* split at 41.1 Ma but much older than the estimated crown age for *Trypodendron* at 11.6 Ma, allowing for the possibility that an ancestral African *Scolytoplatypus* symbiont was horizontally transferred to *Trypodendron.* The estimate for *Phialophoropsis* (5 Ma) postdates the origin of the *Trypodendron* mycangium (11.6 Ma). Likewise, the crown age for the *Toshionella/Ambrosiella* clade (node 4, Fig. 9) at 30.5 Ma allows for an origin of the clade following the African-Asian *Scolytoplatypus* split and horizontal transfer of *Ambrosiella* to the *Xylosandrus* complex. The estimated crown age of *Ambrosiella* including the *Remansus* symbiont (*A. remansi*) (node 5, Fig. 9), is 18.1 Ma, which is older than the estimated origin of the entire tribe *Xyleborini* (including the mesonotum mycangium clade) at 14.3 (Pistone et al. 2018), but the crown of *Ambrosiella* minus *A. remansi* (i.e., the mesonotum mycangium symbionts) is younger at 12 Ma. The estimated crown age of *Meredithiella* (16.6 Ma) closely approximates the purported origin of the prothoracic coil mycangium of *Corthylus* (16.4 Ma according to Gohli et al. 2017), which would be consistent with the hypothesis that this was a third origin of ambrosia symbiosis in the *Ceratocystidaceae* (Mayers et al. 2015, 2018).

ANCESTRAL STATE RECONSTRUCTION

Phylogenetic analyses (Fig. 7) and divergence date comparisons between the fungal symbionts and their respective mycangia (Fig. 9) suggested three evolutionary events leading to ambrosia symbiosis, resulting in three ambrosial clades: *Wolfgangiella/Phialophoropsis*, *Toshionella/Ambrosiella*, and *Meredithiella.* Ancestral state reconstruction further indicated that each of the three groups were likely derived from non-ambrosial ancestors (Fig. 9). For the common ancestor of *Ambrosiella*, *Toshionella*, and *Meredithiella* (node 2, Fig. 9), there was similar support for an ambrosial lifestyle vs a non-ambrosial lifestyle, but the former would require the ambrosial lifestyle to have been reversed at least twice (for *C. adiposa* and *S. norvegica*).

DISCUSSION

This study represents the most comprehensive molecular phylogeny of ambrosia fungi in the *Ceratocystidaceae* and the first to compare the evolutionary history of these fungi to the evolutionary history of their associated mycangia. It is also the

first to fully characterise the mycangia and mycangial symbionts of the ambrosia beetle tribe *Scolytoplatypodini*, which appear central to the origin of ambrosia beetle symbiosis in the *Ceratocystidaceae*. Two novel genera were needed to accommodate the symbionts of *Scolytoplaypus*, raising the number of symbiotic genera in the *Ceratocystidaceae* to five: *Ambrosiella*, *Meredithiella*, *Phialophoropsis*, *Toshionella*, and *Wolfgangiella.* With the exception of *A. remansi*, each genus is strictly associated with a single mycangium type, but there appears to be only limited species-level coevolution within fungal genera. We further propose that the *Scolytoplatypodini* must have domesticated *Ceratocystidaceae* symbionts at least twice, that the *Xylosandrus* complex horizontally acquired their ancestral *Ambrosiella* cultivar from the *Scolytoplatypodini*, and that *Meredithiella* was separately domesticated by *Corthylus.* The origin of *Phialophoropsis* cultivation by *Trypodendron* remains unclear.

The form and evolution of Scolytoplatypodini mycangia

The *Scolytoplatypodini* mycangium was first illustrated by Berger & Cholodkovsky (1916), was hypothesized to carry fungal spores by Nunberg (1951), and described in detail by Schedl (1962). The mycangium is a large, disk-shaped cavity in the prothorax, lined with internal setae that help guide spores through a small conspicuous pore on the dorsal pronotum. The mycangium is surrounded with abundant gland cells whose secretions support the growth of fungal propagules inside the cavity (Schedl 1962, Beaver & Gebhardt 2006). Gross mycangium morphology of the three lineages in the tribe *Scolytoplatypodini* is similar, but we confirm the observation of Schedl (1962) that the interior setae of the mycangia are dramatically different in African and Asian *Scolytoplatypus*. Interestingly, the mycangium of *R. mutabilis* had a third form of setae socketed terminally on cylindrical pedestals, as well as reticulated finger-like cones similar to the reticulated cones of Asian *Scolytoplatypus* but lacking terminal setae. In both *Remansus* and Asian *Scolytoplatypus* the reticulated cones may contain active gland cells because the area between the reticulations stained deeply with cotton blue (implying living cytoplasm) and Berger & Cholodkovsky (1916) illustrated nucleated cells between the reticulations. Alternatively, the cones might serve as channels for glandular secretions from gland cells outside the mycangium wall (Schedl 1962). In either case, the cones may help secreted nutrients penetrate into the dense mass of fungal propagules in the mycangium. The cones may also fill space in the mycangium so that a smaller fungal mass is required to squeeze inoculum from the dorsal pore, which is accomplished by a simple movement of the beetle's head and thorax muscles (Schedl 1962). African *Scolytoplatypus* lack the cones and would appear to have the more primitive mycangium type.

The similarity of the highly developed reticulated mycangium walls and cones in *Remansus* and Asian *Scolytoplatypus*, and the close phylogenetic relationship of their symbionts (*Ambrosiella* and *Toshionella*), could be explained by the two beetle lineages forming a group sister to a more primitive African *Scolytoplatypus*, as implied by Schedl (1975). The mycangium wall of the Asian *S. daimio* was reported by Schedl (1962) to be unreticulated and composed of rigid plates, similar to the sclerotized walls of the African species, and reticulations may be a more advanced character in some but not all Asian species. However, phylogenetic analyses (Jordal 2013, 2018, Gohli et al. 2017, Pistone et al. 2018) place *Remansus* sister to a monophyletic *Scolytoplatypus*. Under this assumption, Asian *Scolytoplatypus* and *Remansus* either:

1. independently and convergently evolved the complex reticulations of their mycangium walls and the reticulated cones; or
2. the African lineage of *Scolytoplatypus* underwent a reduction in mycangium complexity and lost its reticulated cone structures.

Further complicating the matter, *Toshionella* and *Ambrosiella*, the symbionts of the *Scolytoplatypodini* with reticulated cones, appear to be superior ambrosia fungi as they form lush ambrosia growth with large, lipid-filled aleurioconidia and disarticulating conidiophore cells, believed to be advantageous for insect grazing (Nakashima et al. 1992, Harrington et al. 2014, Mayers et al. 2015, 2017). *Wolfgangiella*, the symbiont associated with the simpler African mycangium type, produces less luxuriant ambrosia with columns of relatively small propagules that apparently lack lipid bodies. The tribe *Scolytoplatypodini* likely had an Afro-tropical ancestral origin (Pistone et al. 2018), and only species in the African lineage of *Scolytoplatypus* are found in Africa today (Jordal et al. 2013, 2018). Asian *Scolytoplatypus* are strictly Asian and *Remansus* is known only from Madagascar, where the African lineage of *Scolytoplatypus* is also found. Interestingly, the African species of *Scolytoplatypus* that we studied in Madagascar were associated with the putatively primitive fungal symbiont, *Wolfgangiella*, rather than the *Ambrosiella* symbiont of the sympatric *R. mutabilis*. The absence of *Remansus* and Asian *Scolytoplatypus* from the putative ancestral origin in Africa, the apparently-derived nature of their mycangia, and their closely-related and advanced fungal symbionts would be best explained by these two lineages forming a sister group to a basal African *Scolytoplatypus.* However, this is in conflict with the phylogenetic analyses of the *Scolytoplatypodini*.

Mycangium morphology is often underappreciated in taxonomic treatments of ambrosia beetles. The mycangium setae in *Scolytoplatypus* are one of several morphological traits separating the Asian and African clades of the genus (Schedl 1975, Beaver & Gebhardt 2006, Jordal 2013) and help support a separate genus for the Asian clade (the African *S. permirus* is the type species of *Scolytoplatypus*). The subgenera *Spongocerus* and *Taeniocerus* were previously proposed for Japanese *Scolytoplatypus* spp. and are available, but they were not generally accepted (Wood 1983, Beaver & Gebhardt 2006). Beaver & Gebhardt (2006) list seven Asian *Scolytoplatypus* species that reportedly do not have pronotal mycangium openings in females, and Knížek (2008) described an eighth species. Bright (1994) noted that in one of these species (*S. reticulatus*) the females instead have a smooth, circular spot in place of the mycangium opening. These species are unusual and should be examined further to determine if they represent a true loss of mycangia – which would be novel in ambrosia beetles except for possible analogous cases in a *Camptocerus* subclade that reverted to phloem feeding (Smith 2013) and the mycokleptic *Diuncus* of the *Xylosandrus* complex (Hulcr & Cognato 2010, Skelton et al. 2019) – and if they still obligately feed on fungi through alternative strategies, e.g., as mycokleptics. Otherwise, both the ambrosia beetle lineages and their fungal symbionts appear to be on irreversible evolutionary tracts.

Rejection of a single ancestral ambrosia fungus

Previous phylogenetic analyses showed that the ambrosial genera are interspersed with the non-ambrosial genera *Huntiella*, *Bretziella fagacearum*, *Catunica adiposa*, and *Solaloca norvegica* (De Beer et al. 2014, 2017, Mayers et al. 2015, 2018), and these anomalous placements are more strongly supported in this study. These taxa include wound colonizers (*Huntiella*), plant pathogens (*B. fagacearum* and *C. adiposa*), and a bark beetle associate with an unknown ecological role (*S. norvegica*) (Reid et al. 2010, De Beer et al. 2014). The five ambrosial genera share derived and apparently convergent traits conducive to their role as obligate ambrosia beetle symbionts, including

dimorphic (mycangial and mycelial) forms, easily-grazed conidiophores, dense and pure ambrosia growth in galleries, and (in *Ambrosiella*, *Meredithiella*, and *Toshionella*) large, lipid-filled aleurioconidia.

The non-ambrosial taxa of the *Ceratocystidaceae* with known sexual morphs form long-necked perithecia with sticky ascospore masses at the top to facilitate dispersal on insect exoskeletons (Cain & Weresub 1957, Malloch & Blackwell 1993, Harrington 2009). Surprisingly, the ascomata of *A. cleistominuta* (Mayers et al. 2017), *A. xylebori*, and *W. franznegeri* are neckless (cleistothecia) and lack sticky ascospore drops. Similar immature ascomata in *Meredithiella* were thought to be unfertilized cleistothecia (Mayers et al. 2018). The sexual morph of these ambrosia fungi may be more important in fostering genetic diversity than in dispersal on the exoskeleton, and the ascospores may be eaten and pass through the gut (Mayers et al. 2017). Rather than a cleistothecious ancestor and four reversions from cleistothecia back to necked perithecia, it seems more likely that the ancestors of these ambrosial genera had long-necked perithecia and that neckless ascomata arose convergently in the absence of evolutionary pressure on cuticular dispersal of ascospores.

If the common ancestor of the five ambrosial genera was itself an ambrosia fungus, then the non-ambrosial taxa would need to represent multiple reversions from derived ambrosia beetle mutualists back to free-living species, which has been considered highly unlikely in fungi domesticated for insect agriculture. Possible reversions are not apparent in the ambrosial genus *Raffaelea*, which is polyphyletic and appears to be the result of multiple domestication events (Vanderpool et al. 2018). Escape from symbiosis has not been identified in the cultivars of fungus-farming termites that are specialized to their symbiosis (Aanen et al. 2002, Nobre et al. 2011). Escape from symbiosis may have occurred in some 'lower-attine' cultivars that have no significant adaptation for cultivation and are able to live freely (Vo et al. 2009), but reversions are not seen in the truly domesticated 'higher-attine' cultivars (Schultz & Brady 2008, Mikheyev et al. 2010, Mueller et al. 2018). Cryptic sexual morphs could allow cultivars to more easily escape symbiosis (Mueller 2002, Aanen 2006, Mikheyev et al. 2007, 2010), but in contrast to the widely wind-dispersed basidiospores of the agaric symbionts of both fungus-farming ants (Mueller et al. 2018) and termites (Aanen et al. 2002), the cleistothecious sexual morphs produced by *Ambrosiella* and *Wolfgangiella* are confined to tunnels in wood that are not conducive to independent dispersal.

There are significant morphological differences among the ambrosial genera, most notably the presence of aleurioconidia and the thick ambrosia growth of *Toshionella*, *Ambrosiella*, and *Meredithiella*. In contrast, *Phialophoropsis* and *Wolfgangiella* lack aleurioconidia (as does their nearest neighbour, the non-ambrosial *B. fagacearum*) and have sparser ambrosia growth. *Phialophoropsis* produces relatively unremarkable but quickly-replenished phialoconidia, and *Wolfgangiella* only produces fragmenting arthroconidia, neither of which was observed to have the conspicuous lipid bodies of the genera with aleurioconidia. The ascospores of *Ambrosiella* and *Wolfgangiella*, despite being produced in cleistothecious ascomata, differ significantly in size (those of *Wolfgangiella* are dramatically larger) and shape, further supporting convergent adaptations to neckless cleistothecia. Ancestral state reconstruction also supported a non-ambrosial ancestor for the three clades of ambrosial fungi.

Accepting the estimated divergence dates produced in our analysis, the crown age of tribe *Scolytoplatypodini* (52 Ma by Pistone et al. 2018) is too young to accommodate a single ambrosial common ancestor of both *Wolfgangiella* and *Toshionella* at 62.4 Ma. The ancestral mycangial symbiont of tribe *Scolytoplatypodini* is unclear, and the estimated splits of *Wolfgangiella* and *Phialophoropis* (node 3, Fig. 9) at 31.2 Ma and of *Toshionella* and *Ambrosiella* (node 4, Fig. 9) at 30.5 Ma both follow the split of the African and Asian clades of *Scolytoplatypus* at 41.1 Ma (Pistone et al. 2018). Either a *Toshionella*-like or a *Wolfgangiella*-like symbiont could have been the *Scolytoplatypus* symbiont before the African-Asian split. Regardless, the data at hand suggest that the first *Ceratocystidaceae* farmer was an ancestral *Scolytoplatypodini*.

Conclusions could change if *Platypodinae* ambrosia beetles, a lineage of ambrosia beetles outside of the *Scolytinae* (Mugu et al. 2018), were found to associate with *Ceratocystidaceae* symbionts. The entirely-ambrosial *Platypodinae* may have begun fungus farming at 86 Ma or earlier, long before the fungus-farming ambrosia beetle lineages in *Scolytinae* (Vanderpool et al. 2018). The early *Platypodinae* symbionts probably gave rise to the *Raffaelea* cultivars that dominate the associations with ambrosial *Scolytinae* (Vanderpool et al. 2018). The studied *Platypodinae* have *Raffaelea* as their primary symbionts (Harrington et al. 2010, Li et al. 2018a), but the thick, white ambrosia growth and black rind in galleries of the platyponine *Crossotarsus niponicus* (Nakashima et al. 1987) are notably similar to the ambrosia growth of *Ambrosiella* and *Meredithiella* (Mayers et al. 2015, 2017, 2018). The mycangium of *C. niponicus* is uniquely complex compared to other *Platypodinae* (Nakashima 1975, 1979), and its primary symbiont remains unclear; the yeasts, mucoromycete fungi and molds implicated as its ambrosia symbionts (Nakashima 1971, Nakashima et al. 1987, 1992) may have been misattributed. Regardless, even an older *Ceratocystidaceae* symbiont of *C. niponicus* would not resolve the phylogenetic and morphological conflicts supporting a single domestication in the family *Ceratocystidaceae*.

A single domestication for Ambrosiella and Toshionella

Toshionella and *Ambrosiella* have similar condiophores and aleurioconidia with large lipid bodies, and they form a monophyletic group of ambrosia fungi with a crown age of 30.5 Ma (node 4, Fig. 9). This follows the split of Asian and African *Scolytoplatypus* at 41.1 Ma (Pistone et al. 2018), i.e., the origin of the Asian *Scolytoplatypus* mycangium, which may or may not have harbored a *Toshionella*-like ancestor at that time. *Toshionella* are carried by all studied Asian *Scolytoplatypus*, but the related *Remansus* is found only in Madagascar (Jordal 2013) and *R. mutabilis* was associated with an *Ambrosiella* symbiont rather than a species of *Toshionella*. *Ambrosiella* have otherwise been associated only with members of the *Xylosandrus* complex, an early-diverging lineage of tribe *Xyleborini* (Johnson et al. 2018), a tribe with a crown age of only 14.3 Ma in the estimate of Pistone et al. (2018). We estimated an older *Ambrosiella* crown age at 18.1 Ma with the *R. mutabilis* symbiont (*A. remansi*) included, whereas the clade of *Ambrosiella* associated with the *Xylosandrus* complex had a younger crown age of 12 Ma. A single transfer of an *Ambrosiella* ancestor from tribe *Scolytoplatypodini* (e.g., *Remansus*) to the *Xyleborini* may have prompted the diversification of the monophyletic *Xylosandrus* complex and their mesonotal mycangia (Hulcr & Cognato 2010, Hulcr & Stelinski 2017, Johnson et al. 2018, Skelton et al. 2019), as well as their *Ambrosiella* symbionts (Mayers et al. 2015, 2017, Lin et al. 2017). However, we are severely limited by sequence analysis of the mycangial contents of just a single specimen of *Remansus*, and it is just as likely that *Remanus* obtained its symbiont from the *Xyleborini*, which has been proposed to be Afro-Asian in origin and is now distributed worldwide (Cognato et al. 2011). The evolutionary history of *Toshionella* and *Ambrosiella* remains unclear, but it is reasonable to speculate that they were derived from a single ancestral domestication by *Remansus*, *Scolytoplatypus*, or an ancestral *Scolytoplatypodini*. Study of the mycangia and sym-

bionts of additional species of *Remansus* (Jordal 2013) and Central and South Asian *Scolytoplatypus* (Beaver & Gebhardt 2006, Mandelshtam & Petrov 2010) may prove enlightening, and it may become apparent that *Ambrosiella* and *Toshionella* are part of a continuous spectrum of symbionts rather than two clearly-distinct genera.

A separate origin for Meredithiella

Despite similar aleurioconidia and fairly close phylogenetic placement, *Meredithiella* may not share a common ambrosial ancestor with *Ambrosiella* and *Toshionella*. The clade accommodating these three fungal genera also contains the non-ambrosial taxa *C. adiposa* and *S. norvegica*. A single domestication by the *Scolytoplatypodini* followed by horizontal transfer is problematic because *Meredithiella* are only associated with *Corthylus* (Mayers et al. 2018), a strictly New World genus not thought to have been sympatric with the Old World *Scolytoplatypodini* (Pistone et al. 2018). The estimated divergence of *Meredithiella* and *Ambrosiella* at 46.7 Ma is post-Gondwanan (De Oliveira et al. 2009) and long after the divergence of New World *Corthylini* and Old World *Scolytoplatypodini* at ~ 100 Ma (Pistone et al. 2018). The estimated crown ages of *Meredithiella* and *Corthylus* are quite similar, however, and an independent domestication of *Meredithiella* by *Corthylus* (Mayers et al. 2015) at ~ 16 Ma in the New World is a reasonable hypothesis.

Unstudied genera of *Corthylina* could help support or refute the exclusive association of *Corthylus* with *Meredithiella*. *Amphicranus* may be sister to *Corthylus* (Pistone et al. 2018), but its mycangia and symbionts are unknown. *Microcorthylus* have mycangia similar to those of *Corthylus* (Schedl 1962) and have been associated with *Geosmithia* symbionts (Kolařík & Kirkendall 2010), but mycangial symbionts of *Microcorthylus* have not been confirmed. The well-studied *Corthylina* genera *Gnathotrichus* and *Monarthrum* (Gohli et al. 2017, Johnson et al. 2018) have *Raffaelea* mycangial symbionts (Harrington et al. 2010) and small procoxal mycangia (Francke-Grosmann 1967) that may represent precursors to the *Corthylus* mycangium. Perhaps the domestication of *Meredithiella* replaced a *Raffaelea* cultivar and led to the development of the larger prothoracic coil mycangium of *Corthylus*.

The ambiguous domestications of Wolfgangiella and Phialophoropsis

Wolfgangiella and *Phialophoropsis* lack aleurioconidia and form a monophyletic ambrosial clade that is distantly related to other ambrosia beetle symbionts in the family. *Wolfgangiella* and *Phialophoropsis* are also distantly related to one another and to their closest relative, *Bretziella.* The three genera have no known close relatives and share few common morphological characters, other than the absence of aleurioconidia. The crown age of *Phialophoropsis* and *Wolfgangiella* (node 3, Fig. 9) was estimated at 31.2 Ma in our analysis. One possibility is that *Wolfgangiella* and *Phialophoropsis* are derived from a single domestication, perhaps by African *Scolytoplatypus* after its split from Asian *Scolytoplatypus* at 41.1 Ma (Pistone et al. 2018), which was followed by horizontal transfer to an ancestor of *Trypodendron* (crown age 11.6 Ma, Pistone et al. 2018) in Asia. Genetic diversity in the studied species of *Wolfgangiella* and *Phialophoropsis* is very low, resulting in very young crown age estimates for both genera, but the ITS sequences recovered from mycangia of central African *S. congonus* suggest more diversity (and an older crown age) in *Wolfgangiella* than was found in our multi-gene analyses. Central and Northern African *Scolytoplatypus* (Browne 1971), especially the phylogenetically distinct *S. unipilus* (Jordal 2018), may yield even more divergent symbionts. *Trypodendron* and *Phialophoropsis* have estimated divergence dates at 11.6 Ma and 5 Ma, respectively, which could be consistent with horizontal transfer from African *Scolytoplatypus* or a separate, novel domestication. However, *Trypodendron* is only one of the three ambrosia beetle genera that make up tribe *Xyloterini*, and the crown age for the *Xyloterini* is much older at 50.4 Ma, nearly as old as the estimated crown age of tribe *Scolytoplatypodini* at 53.8 Ma (Pistone et al. 2018). The ambrosia symbionts of the other two *Xyloterini* genera (*Xyloterinus* and *Indocryphalus*) need further study. The distinct mycangia and symbionts of *Xyloterinus* (Abrahamson & Norris 1966, 1969) suggest a much different symbiosis, and the distinct mycangium openings of *Indocryphalus* (Cognato et al. 2015) suggest that its mycangia may differ from those of *Trypodendron*, as may its unstudied ambrosia fungi.

Evolution between Ceratocystidaceae and large mycangia

Despite a wide variety of ubiquitous saprophytes and superficial associates available for domestication, the scolytid ambrosia beetles with large mycangia are only known to be tightly associated with ambrosia fungi in a single family, *Ceratocystidaceae*. These cultivars appear to be derived from at least three novel domestications, despite the ubiquitous presence of earlier-domesticated cultivars of *Raffaelea* s.lat., which have apparently undergone host switching between beetle species, genera, tribes, and subfamilies for more than 80 million years (Vanderpool et al. 2018). *Ceratocystidaceae* ambrosia fungi must provide some superior benefit to their farmers, such as luxuriant ambrosia growth, grazing efficiency, an abundance of specific nutrients, or more effective exclusion of weed fungi. It is noteworthy that the conidiophores and conidia of many of the ambrosia symbionts of the *Ceratocystidaceae* contain an abundance of lipid bodies, and fats (especially sterols such as ergosterol that the insects cannot produce) have been implied as an important nutrient source for bark and ambrosia beetles (Norris et al. 1969, Kok 1979, Six 2003, Bentz & Six 2006). Presumably, the *Ceratocystidaceae* are rich in some beneficial nutrient (Huang et al. 2019) or have another feature that has allowed for multiple mycangium-specific associations over the more common *Raffaelea* spp., or perhaps they are better able to select against or compete with deleterious weed fungi (Castrillo et al. 2016, Ranger et al. 2018).

There must also be a reason that mycangia that carry *Ceratocystidaceae* convergently evolved to be relatively large in relation to the beetles' size and have complex forms such as winding tubes or folded pouches with reticulated glandular walls. *Raffaelea* generally freely associate with different types of small mycangia in unrelated ambrosia beetle species, and multiple *Raffaelea* spp. can co-occur within the mycangia of a single adult beetle (Harrington & Fraedrich 2010, Harrington et al. 2010, 2011, 2014, Li et al. 2018a, Skelton et al. 2018), whereas large mycangia harbour pure cultures of a specific lineage of *Ceratocystidaceae*. These mycangia are 'large' and 'complex', but these aspects alone cannot explain how they selectively maintain strict symbioses with a specific genus of ambrosia fungus. Differential selection of specific *Ambrosiella* cultivars has been demonstrated to occur in mesonotal mycangia (Skelton et al. 2019), and an abundance of gland cells often lines the walls of large mycangia. Specificity is unlikely to be strictly through the action of antifungal or antibacterial secretions because the compounds would have to be exceedingly broad in their targets and potent in their effect while leaving the mycangial symbiont unharmed. It is more likely that some specific nutrient produced by these mycangia is uniquely or preferentially metabolised by *Ceratocystidaceae*, perhaps an unusual amino acid or oil. *Trypodendron* mycangia were shown to be sparsely filled and to carry propagules of weed fungi in the off season, but they were filled to capacity with homogenous masses of fungal propagules when mycangial glands enlarged

and activated (Schneider & Rudinsky 1969). Schneider (1975) observed that in *Trypodendron* and other ambrosia beetles, mycangium gland cells swelled and became activated when fungal propagules entered the mycangium. In response to their secretions, the fungus switched to a mycangial morph and grew and divided to fill the mycangium, which eventually overflowed with fungal propagules. When the beetles were tending the garden or in diapause, the glands became inactive and fungal growth stopped. Some component of the mycangial secretions most likely provides a competitive edge for the growth of *Ceratocystidaceae*, filling the mycangium with their propagules and pushing other fungi out of the mycangium.

Mycangial wall reticulations may be important in reinforcing delicate layers of gland cells, such as those in Asian *Scolytoplatypus*, *Remansus*, *Trypodendron* (Francke-Grosmann 1956, Schneider & Rudinsky 1969), *Corthylus* (Giese 1967, Mayers et al. 2018), and at least *Cnestus* in the *Xylosandrus* complex (Stone et al. 2007). However, African *Scolytoplatypus* mycangia do not have reticulated walls (Schedl 1962). We have also not observed reticulations in the mesonotal mycangia of *Xylosandrus* (Harrington et al. 2014, Mayers et al. 2015) or *Anisandrus* (Mayers et al. 2017), which have a dense concentration of gland cells situated on the part of the scutellum that is contiguous with the mycangium wall (Francke-Grosmann 1963, 1967); in these beetles, the rest of the mycangium wall is thin, transparent, and flexible, and it stretches as the mycangium lobes enlarge with fungal growth (Li et al. 2018b).

Reciprocal co-adaptation and diffuse co-evolution

Fungus farming represents a major evolutionary feature in the *Scolytinae* (Gohli et al. 2017), and mycangia play an essential role in the upkeep, survival, and transmission of vital symbiotic fungi, which are themselves likely under appreciable evolutionary pressure. Mycangia (especially the large organs that carry *Ceratocystidaceae*) and their secretions represent a significant energy investment by the beetle for the long-term maintenance of their domesticated fungal cultivars. Especially in the haplo-diploid *Xyleborini* (Van de Peppel et al. 2018), clonal fungal cultivars appear to be maintained by nearly-exclusive vertical transfer, with some caveats (Skelton et al. 2019). With such obligate mutualism and evolutionary feedback between mycangium secretions and fungal growth, a strict species-level co-evolution might be expected (Mayers et al. 2015). However, patterns of ambrosia beetle symbiosis in general, and with the *Ceratocystidaceae* in particular, appear to be more diffuse. With the exception of *Remansus*, each *Ceratocystidaceae* genus is constrained to a specific mycangium type, yet sympatric beetle species with the same mycangium type sometimes carry the same fungal species, as has been demonstrated here in *Wolfgangiella* and *Toshionella* and previously in *Ambrosiella* (Lin et al. 2017, Skelton et al. 2019), *Meredithiella* (Mayers et al. 2018), and *Phialophoropsis* (Lehenberger et al. 2019). There may be gradients of specificity (i.e., coevolution) and of host-symbiont phylogenetic congruence within these ambrosial clades, as in the well-studied *Ambrosiella*, where host switching is only clearly evident in the basal *A. beaveri* complex and in *A. catenulata* (Lin et al. 2017, Skelton et al. 2019). The secretions of each ambrosia beetle's mycangium may preferentially support growth of its co-evolved fungus but still allow the growth of closely-related species in the absence of competition from the co-evolved symbiont (Skelton et al. 2019).

Reciprical co-adaptation with diffuse co-evolution has been seen in the other fungus-farming insect systems (Nobre et al. 2011, Mueller et al. 2018). Obligate fungus-farming originated in attine ants about 55–65 Ma (Branstetter et al. 2017), and they farm five lineages of fungi in three separate clades of Agaricales (Mueller et al. 2018). Many of the attine ants are farmers of 'lower-attine' cultivars that are closely related and may themselves be free-living fungi (Mueller et al. 2018), but four ant genera (the higher-attines) in a monophyletic sublineage derived from the lower-attine ants farm two sister clades ('Clade-A' and 'Clade-B'). These two clades are truly-domesticated 'higher-attine' fungi and produce 'gongylidia' structures, which are special adaptations for ant grazing that arose an estimated 22–25 Ma (Branstetter et al. 2017, Mueller et al. 2018). Higher-attine ants may farm both higher- and lower-attine cultivars in the same nest (Mueller et al. 2018). The apparent superiority of gongylidia-associated cultivars over lower-attine symbionts (Mueller et al. 2018) is similar to the superiority of domesticated ambrosia fungal cultivars that produce ambrosia growth (e.g., *Ambrosiella* and *Raffaelea*) over undomesticated bark and ambrosia beetle symbionts (Batra 1985, Harrington 2005). Fungus-farming originated in termites about 31 Ma (Roberts et al. 2016), and they farm a single fungal genus, *Termitomyces* (*Agaricales*) (Aanan et al. 2002, Nobre et al. 2010, 2011). Similar to the large mycangium-*Ceratocystidaceae* associations, there is broad but strict lineage-level specificity between termites and their cultivars, but closely-related termite species commonly trade closely-related fungal cultivars (Nobre et al. 2011).

The reciprocal co-adaptation of mycangia and ambrosia fungi, and their irreversible life-styles, presents an intriguing model system for the evolution of obligate mutualisms. Recent studies suggest that patterns of interdependence, specificity, and co-adaptation vary greatly across ambrosia beetle lineages and their fungi, and these patterns may correspond with the diversity of mycangia. Each ambrosia beetle lineage associated with the *Ceratocystidaceae* appears to have originated with a new mycangium and domestication or horizontal transfer of a fungal symbiont. The mycangia and fungi have presumably adapted in response to one another over their shared evolutionary histories, though species-level co-evolution is not readily apparent. In the near future, genomic investigations are likely to provide answers to deeper questions, perhaps concerning metabolic adaptations or losses, host-cultivar signalling, and whether or not there are other molecular signatures of coevolution, on both sides of the symbiosis. Regardless, there remains a uniquely strong fidelity between each type of large and complex mycangium and the genus of its *Ceratocystidaceae* partners.

Acknowledgements The technical assistance of Cinthia Wilkinson, Kyle Small, and Zachary Schultz is greatly appreciated (Iowa State University, ISU). We thank Hisashi Kajimura (Nagoya University) and Caroline Wuest (ISU) for providing cultures; Richard Roeper and Mark Bunce (Alma College) for providing timber worm galleries; James Skelton, You Li, and Jiri Hulcr (University of Florida) for providing ITS sequences; Georg Hausner (University of Manitoba) for providing *C. norvegica* micrographs; and Jostein Gohli and Dario Pistone (University of Bergen) for providing valuable raw data. HCIO (ICAR-Indian Agricultural Research Institute), Royal Botanic Gardens (Kew), and CABI assisted with the lectotypification of *C. adiposa*, and Keith Seifert (AAFC), Adnan Uzunovic (FPInnovations), and Philippe Tanguay (NRCan) with its epitypification. Daniel Young (University of Wisconsin) confirmed the ID of *Elateroides lugubris* and Cletus Kurtzman (USDA ARS) confirmed the ID of *Alloascoidea*. Christopher Werle (USDA ARS) assisted with the collection of *X. compactus* galleries in Mississippi. Chase Mayers was supported in part by a fellowship from the Office of Biotechnology, Iowa State University (ISU). Other financial support was provided by the U.S. Forest Service through cooperative agreements with ISU.

REFERENCES

Aanen DK. 2006. As you reap, so shall you sow: coupling of harvesting and inoculating stabilizes the mutualism between termites and fungi. Biology Letters 2: 209–212.

Aanen DK, Eggleton P, Rouland-Lefevre C, et al. 2002. The evolution of fungus-growing termites and their mutualistic fungal symbionts. Proceedings of the National Academy of Sciences 99: 14887–14892.

Abrahamson LP, Norris DM. 1966. Symbiontic interrelationships between microbes and ambrosia beetles. I. The organs of microbial transport and perpetuation of Xyloterinus politus. Annals of the Entomological Society of America 59: 877–880.

Abrahamson LP, Norris DM. 1969. Symbiontic interrelationships between microbes and ambrosia beetles IV. Ambrosial fungi associated with Xyloterinus politus. Journal of Invertebrate Pathology 14: 381–385.

Agarwal K, Kathuria S, Sundar G, et al. 2014. A case of allergic fungal rhinosinusitis due to Ceratocystis adiposa. Diagnostic Microbiology and Infectious Disease 78: 196–198.

Amselem J, Cuomo CA, Van Kan JA, et al. 2011. Genomic analysis of the necrotrophic fungal pathogens Sclerotinia sclerotiorum and Botrytis cinerea. PLoS Genetics 7: e1002230.

Bateman C, Huang YT, Simmons DR, et al. 2017. Ambrosia beetle Premnobius cavipennis (Scolytinae: Ipini) carries highly divergent ascomycotan ambrosia fungus, Afroraffaelea ambrosiae gen. nov. et sp. nov.(Ophiostomatales). Fungal Ecology 25: 41–49.

Batra LR. 1967. Ambrosia fungi - a taxonomic revision, and nutritional studies of some species. Mycologia 59: 976–1017.

Batra LR. 1985. Ambrosia beetles and their associated fungi: research trends and techniques. Proceedings of the Indian Academy of Science (Plant Sciences) 94: 137–148.

Batra LR, Francke-Grosmann H. 1961. Contributions to our knowledge of ambrosia fungi. I. Ascoidea hylecoeti sp. nov. (Ascomycetes). American Journal of Botany 48: 453–456.

Batra LR, Francke-Grosmann H. 1964. Two new ambrosia fungi: Ascoidea asiatica and A. africana. Mycologia 56: 632–636.

Beaver RA. 1989. Insect-fungus relationships in the bark and ambrosia beetles. In: Wilding N, Collins NM, Hammond PM, et al. (eds), Insect-fungus interactions: 121–143. Academic Press, United Kingdom.

Beaver RA, Gebhardt H. 2006. A review of the Oriental species of Scolytoplatypus Schaufuss (Coleoptera, Curculionidae, Scolytinae). Deutsche Entomologische Zeitschrift 53: 155–178.

Beimforde C, Feldberg K, Nylinder S, et al. 2014. Estimating the Phanerozoic history of the Ascomycota lineages: combining fossil and molecular data. Molecular Phylogenetics and Evolution 78: 386–398.

Bentz BJ, Six DL. 2006. Ergosterol content of fungi associated with Dendroctonus ponderosae and Dendroctonus rufipennis (Coleoptera: Curculionidae, Scolytinae). Annals of the Entomological Society of America 99: 189–194.

Berbee ML, Taylor JW. 2010. Dating the molecular clock in fungi – how close are we? Fungal Biology Reviews 24: 1–6.

Berger VM, Cholodkovsky NA. 1916. On some points of biology and anatomy of the genus Scolytoplatypus Blandford (Coleoptera, Ipidae). Revue Russe d'Entomologie 16: 1–7.

Bhat VR. 1972. Observations on Ceratocystis adiposa and the conidial ontogeny of its imperfect stabe. Sydowia Annales Mycologici 26: 26–28.

Bouckaert R, Heled J, Kühnert D, et al. 2014. BEAST 2: a software platform for Bayesian evolutionary analysis. PLoS Computational Biology 10: e1003537.

Brader L. 1964. Étude de la relation entre le scolyte des rameaux du caféir, Xyleborus compactus Eichh. (X. morstatti Hag.), et sa plante-hôte. Mededelingen van de Landbouwhogeschool Wageningen, Nederland 64: 1–109.

Branstetter MG, Ješovnik A, Sosa-Calvo J, et al. 2017. Dry habitats were crucibles of domestication in the evolution of agriculture in ants. Proceedings of the Royal Society B 284: 20170095.

Bright DE. 1994. New records and new species of Scolytidae from Borneo (Coleoptera: Scolytidae). Koleopterologische Rundschau 64: 257–274.

Browne FG. 1971. The African species of Scolytoplatypus Schaufuss (Coleoptera, Scolytidae). Revue de Zoologie et de Botanique Africaines 84: 111–129.

Butler EJ. 1906. Fungus diseases of sugar-cane in Bengal. Memoirs of the Department of Agriculture in India 1, No. 3: 1–53 (plus nine unpaginated plates).

Cain RF, Weresub LK. 1957. Studies of coprophilous ascomycetes: V. Sphaeronaemella fimigola. Canadian Journal of Botany 35: 119–131.

Castrillo LA, Griggs MH, Vandenberg JD. 2016. Competition between biological control fungi and fungal symbionts of ambrosia beetles Xylosandrus crassiusculus and X. germanus (Coleoptera: Curculionidae): Mycelial interactions and impact on beetle brood production. Biological Control 103: 138–146.

Cognato AI, Hulcr J, Dole SA, et al. 2011. Phylogeny of haplo-diploid, fungus-growing ambrosia beetles (Curculionidae: Scolytinae: Xyleborini) inferred from molecular and morphological data. Zoologica Scripta 40: 174–186.

Cognato AI, Jordal BH, Rubinoff D. 2018. Ancient 'wanderlust' leads to diversification of endemic hawaiian Xyleborus species (Coleoptera: Curculionidae: Scolytinae). Insect Systematics and Diversity 2: 1.

Cognato AI, Smith SM, Pham TH. 2015. Cladistic analysis of Indocryphalus Eggers (Coleoptera: Curculionidae: Scolytinae: Xyloterini) and description of a new species from Vietnam. Insect Systematics and Evolution 46: 493–506. doi: https://doi.org/10.1163/1876312X-46052129.

Davidson RW. 1935. Fungi causing stain in logs and lumber in the Southern States, including five new species. Journal of Agricultural Research 50: 789–807.

De Beer ZW, Duong TA, Barnes I, et al. 2014. Redefining Ceratocystis and allied genera. Studies in Mycology 79: 187–219.

De Beer ZW, Marincowitz S, Duong TA, et al. 2017. Bretziella, a new genus to accommodate the oak wilt fungus, Ceratocystis fagacearum (Microascales, Ascomycota). MycoKeys 27: 1–19.

De Oliveira FB, Molina EC, Marroig G. 2009. Paleogeography of the South Atlantic: a route for primates and rodents into the New World? In: Garber PE, Estrada A, Bicca-Marques JC, et al. (eds), South American primates: 55–68. Springer, USA.

Dreaden TJ, Davis JM, De Beer ZW, et al. 2014. Phylogeny of ambrosia beetle symbionts in the genus Raffaelea. Fungal Biology 118: 970–978.

Duvaux L, Shiller J, Vandeputte P, et al. 2017. Draft genome sequence of the human-pathogenic fungus Scedosporium boydii. Genome Announcements 5: e00871-17.

Elwood HJ, Olsen GJ, Sogin ML. 1985. The small-subunit ribosomal RNA gene sequences from the hypotrichous ciliates Oxytricha nova and Stylonychia pustulata. Molecular Biology and Evolution 2: 399–410.

Farrell BD, Sequeira AS, O'Meara BC, et al. 2001. The evolution of agriculture in beetles (Curculionidae: Scolytinae and Platypodinae). Evolution 55: 2011–2027.

Francke-Grosmann H. 1956. Hautdrüsen als träger der pilzsymbiose bei ambrosiakäfern. Zeitschrift für Morphologie und Ökologie der Tiere 45: 275–308.

Francke-Grosmann H. 1963. Some new aspects in forest entomology. Annual Review of Entomology 8: 415–438.

Francke-Grosmann H. 1967. Ectosymbiosis in wood-inhabiting insects. In: Henry SM (ed), Symbiosis: 141–206. Academic Press, USA.

Gardes M, Bruns TD. 1993. ITS primers with enhanced specificity for basidiomycetes-application to the identification of mycorrhizae and rusts. Molecular Ecology 2: 113–118.

Gernhard T. 2008. The conditioned reconstructed process. Journal of Theoretical Biology 253: 769–778.

Giese RL. 1967. The Columbian timber beetle, Corthylus columbianus (Coleoptera: Scolytidae). V. A description of the mycetangia. The Canadian Entomologist 99: 54–58.

Glass NL, Donaldson GC. 1995. Development of primer sets designed for use with the PCR to amplify conserved genes from filamentous ascomycetes. Applied and Environmental Microbiology 61: 1323–1330.

Gohli J, Kirkendall LR, Smith SM, et al. 2017. Biological factors contributing to bark and ambrosia beetle species diversification. Evolution 71: 1258–1272.

Greco EB, Wright MG. 2015. Ecology, biology, and management of Xylosandrus compactus (Coleoptera: Curculionidae: Scolytinae) with emphasis on coffee in Hawaii. Journal of Integrated Pest Management 6: 7.

Guindon S, Dufayard JF, Lefort V, et al. 2010. New algorithms and methods to estimate maximum-likelihood phylogenies: assessing the performance of PhyML 3.0. Systematic Biology 59: 307–321.

Hadley A. 2010. CombineZP. Program distributed by the author. Available 2016: http://www.hadleyweb.pwp.blueyonder.co.uk/.

Harrington TC. 2005. Ecology and evolution of mycophagous bark beetles and their fungal partners. In: Vega FE, Blackwell M (eds), Insect-fungal associations: ecology and evolution: 257–291. Oxford University Press, USA.

Harrington TC. 2009. The genus Ceratocystis. Where does the oak wilt fungus fit? In: Appel DN, Billings RF (eds), Proceedings of the 2nd National Oak Wilt Symposium: 21–35. Texas Forest Service Publication, USA.

Harrington TC, Aghayeva DN, Fraedrich SW. 2010. New combinations in Raffaelea, Ambrosiella, and Hyalorhinocladiella, and four new species from the redbay ambrosia beetle, Xyleborus glabratus. Mycotaxon 111: 337–361.

Harrington TC, Fraedrich SW. 2010. Quantification of propagules of the laurel wilt fungus and other mycangial fungi from the redbay ambrosia beetle, Xyleborus glabratus. Phytopathology 100: 1118–1123.

Harrington TC, McNew D, Mayers C, et al. 2014. Ambrosiella roeperi sp. nov. is the mycangial symbiont of the granulate ambrosia beetle, Xylosandrus crassiusculus. Mycologia 106: 835–845.

Harrington TC, Wingfield, MJ. 1998. The Ceratocystis species on conifers. Canadian Journal of Botany 76: 1446–1457.

Harrington TC, Yun HY, Lu SS, et al. 2011. Isolations from the redbay ambrosia beetle, Xyleborus glabratus, confirm that the laurel wilt pathogen, Raffaelea lauricola, originated in Asia. Mycologia 103: 1028–1036.

Hausner G, Reid J. 2004. The nuclear small subunit ribosomal genes of Sphaeronaemella helvellae, Sphaeronaemella fimicola, Gabarnaudia betae, and Cornuvesica falcata: phylogenetic implications. Canadian Journal of Botany 82: 752–762.

Hawes CR, Beckett A. 1977a. Conidium ontogeny in the Chalara state of Ceratocystis adiposa: I. Light microscopy. Transactions of the British Mycological Society 68: 259–265.

Hawes CR, Beckett A. 1977b. Conidium ontogeny in the Chalara state of Ceratocystis adiposa: II. Electron microscopy. Transactions of the British Mycological Society 68: 267–276.

Huang YT, Skelton J, Hulcr J. 2019. Multiple evolutionary origins lead to diversity in the metabolic profiles of ambrosia fungi. Fungal Ecology 38: 80–88.

Hulcr J, Cognato AI. 2010. Repeated evolution of crop theft in fungus-farming ambrosia beetles. Evolution 64: 3205–3212.

Hulcr J, Stelinski LL. 2017. The ambrosia symbiosis: from evolutionary ecology to practical management. Annual Review of Entomology 62: 285–303.

Hunt J. 1956. Taxonomy of the genus Ceratocystis. Lloydia 19: 1–58.

Hutchinson SA. 1939. Macroconidial formation in Ophiostoma majus (van Beyma) Goidanich. Annals of Botany 3: 795–802.

Ito M, Kajimura H. 2017. Landscape-scale genetic differentiation of a mycangial fungus associated with the ambrosia beetle, Xylosandrus germanus (Blandford) (Curculionidae: Scolytinae) in Japan. Ecology and Evolution 7: 9203–9221.

Johnson AJ, McKenna DD, Jordal BH, et al. 2018. Phylogenomics clarifies repeated evolutionary origins of inbreeding and fungus farming in bark beetles (Curculionidae, Scolytinae). Molecular Phylogenetics and Evolution 127: 229–238.

Jordal BH. 2013. Deep phylogenetic divergence between Scolytoplatypus and Remansus, a new genus of Scolytoplatypodini from Madagascar (Coleoptera, Curculionidae, Scolytinae). ZooKeys 352: 9–33.

Jordal BH. 2018. The smallest known species of Afrotropical Scolytoplatypus Schaufuss (Curculionidae, Scolytinae) – with unique features and an isolated phylogenetic position. Zookeys 749: 125–130.

Jordal BH, Cognato AI. 2012. Molecular phylogeny of bark and ambrosia beetles reveals multiple origins of fungus farming during periods of global warming. BMC Evolutionary Biology 12: 133.

Jordal BH, Normark BB, Farrell BD. 2000. Evolutionary radiation of an inbreeding haplodiploid beetle lineage (Curculionidae, Scolytinae). Biological Journal of the Linnean Society 71: 483–499.

Kasson MT, O'Donnell K, Rooney AP, et al. 2013. An inordinate fondness for Fusarium: phylogenetic diversity of fusaria cultivated by ambrosia beetles in the genus Euwallacea on avocado and other plant hosts. Fungal Genetics and Biology 56: 147–157.

Kasson MT, Wickert KL, Stauder CM, et al. 2016. Mutualism with aggressive wood-degrading Flavodon ambrosius (Polyporales) facilitates niche expansion and communal social structure in Ambrosiophilus ambrosia beetles. Fungal Ecology 23: 86–96.

Kinuura H. 1995. Symbiotic fungi associated with ambrosia beetles. Japan Agricultural Research Quarterly 29: 57–63.

Kinuura H, Hijii N, Kanamitsu K. 1991. Symbiotic fungi associated with the ambrosia beetle, Scolytoplatypus mikado Blandford (Coleoptera: Scolytidae) – succession of the flora and fungal phases in the gallery system and the mycangium in relation to the developmental stages of the beetle. Journal of the Japanese Forestry Society 73: 197–205.

Kirkendall LR, Biedermann PH, Jordal BH. 2015. Evolution and diversity of bark and ambrosia beetles. In: Vega FE, Hofstetter RW (eds), Bark beetles: biology and ecology of native and invasive species: 85–156. Academic Press, USA.

Knížek M. 2008. A new species of Scolytoplatypus (Coleoptera: Scolytidae) from China. Studies and reports of District Museum Prague-East Taxonomical Series 4: 119–124.

Kok LT. 1979. Lipids of ambrosia fungi and the life of mutualistic beetles. In: Batra LR (ed), Insect-fungus symbiosis: nutrition, mutualism and commensalism: 33–52. Wiley, USA.

Kolařík M, Kirkendall LR. 2010. Evidence for a new lineage of primary ambrosia fungi in Geosmithia Pitt (Ascomycota: Hypocreales). Fungal Biology 114: 676–689.

Kurtzman CP, Robnett CJ. 2013. Alloascoidea hylecoeti gen. nov., comb. nov., Alloascoidea africana comb. nov., Ascoidea tarda sp. nov., and Nadsonia starkeyi-henricii comb. nov., new members of the Saccharomycotina (Ascomycota). FEMS Yeast Research 13: 423–432.

Lanfear R, Calcott B, Ho SY, et al. 2012. PartitionFinder: combined selection of partitioning schemes and substitution models for phylogenetic analyses. Molecular Biology and Evolution 29: 1695–1701.

Lanfear R, Frandsen PB, Wright AM, et al. 2016. PartitionFinder 2: new methods for selecting partitioned models of evolution for molecular and morphological phylogenetic analyses. Molecular Biology and Evolution 34: 772–773.

Lehenberger M, Biedermann PHW, Benz JP. 2019. Molecular identification and enzymatic profiling of Trypodendron (Curculionidae: Xyloterini) ambrosia beetle-associated fungi of the genus Phialophoropsis (Microascales: Ceratocystidaceae). Fungal Ecology 38: 89–97.

Li Y, Huang YT, Kasson MT, et al. 2018a. Specific and promiscuous ophiostomatalean fungi associated with Platypodinae ambrosia beetles in the southeastern United States. Fungal Ecology 35: 42–50.

Li Y, Ruan Y, Kasson MT, et al. 2018b. Structure of the ambrosia beetle (Coleoptera: Curculionidae) mycangia revealed through micro-computed tomography. Journal of Insect Science 18: 13.

Li Y, Ruan Y, Stanley EL, et al. 2019. Plasticity of mycangia in Xylosandrus ambrosia beetles. Insect Science 26: 732–742.

Lin YT. 2016. The symbiotic fungi of ambrosia beetles with mesothoracic mycangium in Taiwan. MS thesis, National Chung Hsing University, Department of Plant Pathology, Taichung City, Taiwan.

Lin YT, Shih HH, Hulcr J, et al. 2017. Ambrosiella in Taiwan including one new species. Mycoscience 58: 242–252.

Maheswari CU, Sharma RK, Kamil D, et al. 2012. Herbarium Cryptogamae Indiae Orientalis (HCIO): Catalogue of fungal specimens, Volume 1. Indian Agriculatural Research Institute, New Delhi, India.

Malloch D, Blackwell M. 1993. Dispersal biology of the ophiostomatoid fungi. In: Wingfield MJ, Seifert KA, Webber JF (eds), Ceratocystis and Ophiostoma: taxonomy, ecology and pathology: 195–206. APS Press, USA.

Mandelshtam MY, Petrov AV. 2010. Description of new Dryocoetes (Coleoptera, Curculionidae, Scolytinae) species from Afghanistan and Northern India and redescription of Scolytoplatypus kunala Strohm. ZooKeys 56: 179–190.

Marincowitz S, Duong TA, De Beer ZW, et al. 2015. Cornuvesica: A little known mycophilic genus with a unique biology and unexpected new species. Fungal Biology 119: 615–630.

Mathiesen-Käärik A. 1953. Eine Übersicht über die gewöhnlichsten mit Borkenkäfern assoziierten Bläuepilze in Schweden und einige für Schweden neue Bläuepilze. Meddelanden fran Statens Skogsforskningsinstitut 43: 1–74.

Mayers CG, Bateman CC, Harrington TC. 2018. New Meredithiella species from mycangia of Corthylus ambrosia beetles suggest genus-level coadaptation but not species-level coevolution. Mycologia 110: 63–78.

Mayers CG, Harrington TC, Ranger CM. 2017. First report of a sexual state in an ambrosia fungus: Ambrosiella cleistominuta sp. nov. associated with the ambrosia beetle Anisandrus maiche. Botany 95: 503–512.

Mayers CG, McNew DL, Harrington TC, et al. 2015. Three genera in the Ceratocystidaceae are the respective symbionts of three independent lineages of ambrosia beetles with large, complex mycangia. Fungal Biology 119: 1075–1092.

Mikheyev AS, Mueller UG, Abbot P. 2010. Comparative dating of attine ant and lepiotaceous cultivar phylogenies reveals coevolutionary synchrony and discord. The American Naturalist 175: E126–E133.

Mikheyev AS, Mueller UG, Boomsma JJ. 2007. Population genetic signatures of diffuse co-evolution between leaf-cutting ants and their cultivar fungi. Molecular Ecology 16: 209–216.

Moreau C. 1952. Coexistence des formes Thielaviopsis et Graphium chez une souche de Ceratocystis major (van Beyma) nov. comb. Remarques sur les variations des Ceratocystis. Revue de Mycologie (Suppl. Colonial) 17: 17–25.

Mueller UG. 2002. Ant versus fungus versus mutualism: ant-cultivar conflict and the deconstruction of the attine ant-fungus symbiosis. The American Naturalist 160: S67–S98.

Mueller UG, Kardish MR, Ishak HD, et al. 2018. Phylogenetic patterns of ant–fungus associations indicate that farming strategies, not only a superior fungal cultivar, explain the ecological success of leafcutter ants. Molecular Ecology 27: 2414–2434.

Mugu S, Pistone D, Jordal BH. 2018. New molecular markers resolve the phylogenetic position of the enigmatic wood-boring weevils Platypodinae (Coleoptera: Curculionidae). Arthropod Systematics and Phylogeny 76: 45–58.

Nag Raj TR, Kendrick B. 1975. A monograph of Chalara and allied genera. Wilfrid Laurier University Press, Waterloo, Canada.

Nakashima T. 1971. Notes on the associated fungi and the mycetangia of the ambrosia beetle, Crossotarsus niponicus Blandford (Coleoptera: Platypodidae). Applied Entomology and Zoology 6: 131–137.

Nakashima T. 1975. Several types of the mycetangia found in platypodid ambrosia beetles (Coleoptera: Platypodidae). Insecta Matsumurana 7: 1–69.

Nakashima T. 1979. Notes on the time when the new female adults of the ambrosia beetle Crossotarsus niponicus Blandford (Coleoptera: Platypodidae) harvest their symbiotic fungi into their mycetangia. Insecta Matsumurana 17: 1–9.

Nakashima T. 1989. Observation on the ambrosia fungus Ambrosiella sp., growing in the gallery of Scolytoplatypus shogun Blandford (Coleoptera: Scolytidae) and on the concurrent damage of wood tissue. Journal of the Faculty of Agriculture, Hokkaido University 64: 99–105.

Nakashima T, Goto C, Iizuka T. 1987. The primary and auxiliary ambrosia fungi isolated from the ambrosia beetles, Scolytoplatypus shogun Blandford (Coleoptera: Scolytidae) and Crossotarsus niponicus Blandford (Coleoptera: Platypodidae). Journal of the Faculty of Agriculture, Hokkaido University 63: 185–208.

Nakashima T, Otomo T, Owada Y, et al. 1992. SEM observations on growing conditions of the fungi in the galleries of several ambrosia beetles: (Coleoptera: Scolytidea and Platypodidae). Journal of the Faculty of Agriculture, Hokkaido University 65: 239–273.

Nel WJ, Duong TA, Wingfield BD, et al. 2017. A new genus and species for the globally important, multihost root pathogen Thielaviopsis basicola. Plant Pathology 67: 871–882.

Nobre T, Koné NA, Konaté S, et al. 2011. Dating the fungus-growing termites' mutualism shows a mixture between ancient codiversification and recent symbiont dispersal across divergent hosts. Molecular Ecology 20: 2619–2627.

Nobre T, Rouland-Lefèvre C, Aanen DK. 2010. Comparative biology of fungus cultivation in termites and ants. In: Bignell D, Roisin Y, Lo N (eds), Biology of termites: a modern synthesis: 193–210. Springer, Netherlands.

Norris DM, Baker JM, Chu HM. 1969. Symbiontic interrelationships between microbes and ambrosia beetles. III. Ergosterol as the source of sterol to the insect. Annals of the Entomological Society of America 62: 413–414.

Nunberg M. 1951. Contribution to the knowledge of prothoracic glands of Scolytidae and Platypodidae (Coleoptera). Annales Musei Zoologici Polonici 14: 261–267.

O'Donnell K, Sink S, Libeskind-Hadas R, et al. 2015. Discordant phylogenies suggest repeated host shifts in the Fusarium–Euwallacea ambrosia beetle mutualism. Fungal Genetics and Biology 82: 277–290.

Oliveira LS, Harrington TC, Ferreira MA, et al. 2015. Species or genotypes? Reassessment of four recently described species of the Ceratocystis wilt pathogen, Ceratocystis fimbriata, on Mangifera indica. Phytopathology 105: 1229–1244.

Paulin-Mahady AE, Harrington TC, McNew D. 2002. Phylogenetic and taxonomic evaluation of Chalara, Chalaropsis, and Thielaviopsis anamorphs associated with Ceratocystis. Mycologia 94: 62–72.

Pel HJ, De Winde JH, Archer DB, et al. 2007. Genome sequencing and analysis of the versatile cell factory Aspergillus niger CBS 513.88. Nature Biotechnology 25: 221–231.

Pistone D, Gohli J, Jordal BH. 2018. Molecular phylogeny of bark and ambrosia beetles (Curculionidae: Scolytinae) based on 18 molecular markers. Systematic Entomology 43: 387–406.

Rambaut A, Suchard MA, Xie D, et al. 2014. Tracer v. 1.6, available from https://beast.community/tracer.

Ranger CM, Biedermann PH, Phuntumart V, et al. 2018. Symbiont selection via alcohol benefits fungus farming by ambrosia beetles. Proceedings of the National Academy of Sciences 115: 4447–4452.

Rayner RW. 1970. A mycological colour chart. Commonwealth Mycological Institute, Kew, Surrey.

Rehner SA, Samuels GJ. 1994. Taxonomy and phylogeny of Gliocladium analysed from nuclear large subunit ribosomal DNA sequences. Mycological Research 98: 625–634.

Reid J, Iranpour M, Rudski SM, et al. 2010. A new conifer-inhabiting species of Ceratocystis from Norway. Botany 88: 971–983.

Roberts EM, Todd CN, Aanen DK, et al. 2016. Oligocene termite nests with in situ fungus gardens from the Rukwa Rift Basin, Tanzania, support a Paleogene African origin for insect agriculture. PloS One 11: e0156847.

Ronquist F, Teslenko M, Van der Mark P, et al. 2012. MrBayes 3.2: efficient Bayesian phylogenetic inference and model choice across a large model space. Systematic Biology 61: 539–542.

Sartoris GB. 1927. A cytological study of Ceratostomella adiposum (Butl.) comb. nov., the black-rot fangus of sugar-cane. Journal of Agricultural Research 35: 577–583.

Schedl KE. 1975. Die Unterfamilie Scolytoplatypinae (Coleoptera, Scolytoidea). 307 Beitrag zur Morphologie und Systematik der Scolytoides. Entomologische Abhandlungen Staatlisches Museum für Tierkunde in Dresden 40: 199–267.

Schedl W. 1962. Ein Beitrag zur Kenntnis der Pilzübertragungsweise bei xylomycetophagen Scolytiden (Coleoptera). In: Sitzungsberichten der Österreichische Akademie der Wissenschaften: 376–378. Springer, Germany.

Schenk JJ. 2016. Consequences of secondary calibrations on divergence time estimates. PLoS One 11: e0148228.

Schmidberger J. 1836. Naturgeschichte des Apfelborkenkäfers Apate dispar. Beitrage zur Obstbaumzucht und zur Naturgeschichte der den Obstbäumen schädlichen Insekten 4: 213–230.

Schneider I. 1975. Untersuchungen uber die biologische Bedeutung der Mycetangien bei einigen Ambrosiakafern. Material und Organismen 3: 489–497.

Schneider I, Rudinsky JA. 1969. Anatomical and histological changes in internal organs of adult Trypodendron lineatum, Gnathotrichus retusus, and G. sulcatus (Coleoptera: Scolytidae). Annals of the Entomological Society of America 62: 995–1003.

Schoch CL, Seifert KA, Huhndorf S, et al. 2012. Nuclear ribosomal internal transcribed spacer (ITS) region as a universal DNA barcode marker for fungi. Proceedings of the National Academy of Sciences 109: 6241–6246.

Schultz TR, Brady SG. 2008. Major evolutionary transitions in ant agriculture. Proceedings of the National Academy of Sciences 105: 5435–5440.

Simmons DR, Li Y, Bateman CC, et al. 2016. Flavodon ambrosius sp. nov., a basidiomycetous mycosymbiont of Ambrosiodmus ambrosia beetles. Mycotaxon 131: 277–285.

Six DL. 2003. Bark beetle-fungus symbioses. In: Bourtzis K, Miller TA (eds), Insect symbioses: 99–116. CRC Press, USA.

Skelton J, Jusino MA, Li Y, et al. 2018. Detecting symbioses in complex communities: the fungal symbionts of bark and ambrosia beetles within Asian pines. Microbial Ecology 76: 839–850.

Skelton J, Johnson AJ, Jusino MA, et al. 2019. A selective fungal transport organ (mycangium) maintains coarse phylogenetic congruence between fungus-farming ambrosia beetles and their symbionts. Proceedings of the Royal Society B 286: 20182127.

Smith SM. 2013. Phylogenetics of the Scolytini (Coleoptera: Curculionidae: Scolytinae) and host-use evolution. PhD thesis, Department of Entomology, Michigan State University, Lansing, USA.

Stone WD, Nebeker TE, Monroe WA, et al. 2007. Ultrastructure of the mesonotal mycangium of Xylosandrus mutilatus (Coleoptera: Curculionidae). Canadian Journal of Zoology 85: 232–238.

Surina B, Pfanzelt S, Einzmann HJ, et al. 2014. Bridging the Alps and the Middle East: evolution, phylogeny and systematics of the genus Wulfenia (Plantaginaceae). Taxon 63: 843–858.

Swofford DL. 2002. PAUP 4.0 b10: Phylogenetic analysis using parsimony. Sinauer Associates, Sunderland, MA.

Talbot P. 1956. New and interesting records of South African fungi. Part II. Bothalia 6: 489–500.

Upadhyay HP. 1981. A monograph of Ceratocystis and Ceratocystiopsis. University of Georgia Press, Athens, GA, USA.

Van de Peppel LJ, Aanen DK, Biedermann PH. 2018. Low intraspecific genetic diversity indicates asexuality and vertical transmission in the fungal cultivars of ambrosia beetles. Fungal Ecology 32: 57–64.

Van der Nest MA, Bihon W, De Vos L, et al. 2014. Draft genome sequences of Diplodia sapinea, Ceratocystis manginecans, and Ceratocystis moniliformis. IMA Fungus 5: 135–140.

Van der Nest MA, Steenkamp ET, McTaggart AR, et al. 2015. Saprophytic and pathogenic fungi in the Ceratocystidaceae differ in their ability to metabolize plant-derived sucrose. BMC Evolutionary Biology 15: 273.

Vanderpool D, Bracewell RR, McCutcheon JP. 2018. Know your farmer: ancient origins and multiple independent domestications of ambrosia beetle fungal cultivars. Molecular Ecology 27: 2077–2094.

Vilgalys R, Hester M. 1990. Rapid genetic identification and mapping of enzymatically amplified ribosomal DNA from several Cryptococcus species. Journal of Bacteriology 172: 4238–4246.

Vo TL, Mueller UG, Mikheyev AS. 2009 Free-living fungal symbionts (Lepiotaceae) of fungus-growing ants (Attini: Formicidae). Mycologia 101: 206–210.

Von Arx JA, Hennebert GL. 1965. Deux champignons ambrosia. Mycopathologia et Mycologia Applicata 25: 309–315.

White TJ, Bruns T, Lee S, et al. 1990. Amplification and direct sequencing of fungal ribosomal RNA genes for phylogenetics. In: Innis MA, Gelfand DH, Sninsky JJ, et al. (eds), PCR Protocols: a sequencing guide to methods and applications: 315–322. Academic Press, USA.

Wingfield BD, Ambler JM, Coetzee M, et al. 2016a. Draft genome sequences of Armillaria fuscipes, Ceratocystiopsis minuta, Ceratocystis adiposa, Endoconidiophora laricicola, E. polonica and Penicillium freii DAOMC 242723. IMA Fungus 7: 217–227.

Wingfield BD, Duong TA, Hammerbacher A, et al. 2016b. Draft genome sequences for Ceratocystis fagacearum, C. harringtonii, Grosmannia penicillata, and Huntiella bhutanensis. IMA Fungus 7: 317–323.

Wood S. 1983. New synonymy and new species of American bark beetles (Coleoptera: Scolytidae), Part IX. The Great Basin Naturalist 31: 647–659.

Supplementary material

Table S1 GenBank accesions for other ITS sequences used in analyses.

Table S2 GenBank accession numbers for sequences used in multi-locus analyses.

Fig. S1 Asexual morphology of *Catunica adiposa*. a. Chain of conidia produced from phialidic conidiophore; b. detached, pigmented and unpigmented

conidia; c–e. basipetal aleurioconidia with membranous sheaths (a–b. isolate C871 (CBS 600.74) from Japan; c. isolate C906 (CBS 138.34) from The Netherlands; d–e. isolate C299 from USA). — Scale bars = 10 µm.

Fig. S2 HCIO 3531, designated as lectotype for *Catunica adiposa* (= *Sphaeronema adiposum*). a. Specimen label, which reads: '*Sphaeronema adiposum* Butl.', 'on *Saccharum officinarum*', 'Seeraha, Champaran, Bihar', 'Oct. 30th 1903', and 'E.J. Butler'; b. *Saccharum officinarum* infected with *Catunica adiposa*; photographs courtesy of, and reproduced with permission from, Herbarium Cryptogamae Indiae Orientalis (HCIO), Division of Plant Pathology, ICAR-Indian Agricultural Research Institute, New Delhi, India.

Fig. S3 Contents of specimens IMI 21355 (a) and IMI 21285 (b) of *Catunica adiposa* held by Royal Botanic Gardens Kew, the only known alternatives to HCIO 3531 to serve as type for the species. Nag Raj & Kendrick (1975) cited IMI 21355 as holotype for *C. adiposa* without explanation. IMI 21355 consists of dried cultures isolated from sugarcane in India on an uncertain date and prepared slides. This specimen was deposited to the Imperial Bureau of Mycology on 15 January 1927 by W. McRae, the then-Imperial Mycologist of India and a colleague of E.J. Butler's. A letter included by McRae, which probably explained the specific origin of the material, could not be located (pers. comm., CABI and Royal Botanic Gardens, Kew). The available collection information for the specimen (ex sugarcane in Pusa) matches Butler's original description, and presumably McRae was familiar with appropriate material to submit as representative of the species. Handwritten notes on envelopes and slides suggest that IMI 21355 was examined by Sartoris (1927), Hunt (1956), and Nag Raj & Kendrick (1975). IMI 21285 includes envelopes labelled 'type' and 'ex-type', but this specimen was not published as type material and was collected in England decades after the species description (pers. comm., CABI and Royal Botanic Gardens, Kew). Photographs courtesy of, and reproduced with permission from, CABI and Royal Botanic Gardens, Kew.

Fig. S4 Time-calibrated tree produced by secondary-calibrated analysis in BEAST of the six-gene tree dataset (18S rDNA, 28S rDNA, *tef*1-α, *tub*, *mcm7*, and *rpl1*) with median node ages (Analysis A). Horizontal bars indicate 95 % Highest Posterior Density (HPD) ranges. Branch support values are Bayesian posterior probability from BEAST analysis. Scale in millions of years ago (Ma). *Aspergillus niger* was used as the outgroup.